All these findings support for the importance of TTR in prevention of Aβ aggregation and toxicity. However, a role for TTR in Aβ deposition is not yet known. To investigate the relationship between TTR and Aβ deposition, we generated a mouse line carrying a null mutation at the endogenous *TTR* locus and the human mutant amyloid precursor protein (APP) cDNA responsible for familial AD (Tg2576/$TTR^{-/-}$ mouse), by crossing Tg2576 mice with TTR-deficient mice generated through gene targeting (9). We asked whether Aβ deposition was accelerated in Tg2576/$TTR^{-/-}$ mice relative to the heterozygous mutant Tg2576 (Tg2576/$TTR^{+/-}$) mice.

METHODS

Animals

Transgenic mice producing human variant APP and lacking endogenous mouse TTR were generated as follows. A male Tg2576 mouse (13) carrying the human mutant APP cDNA with the double mutation K670N and M671L responsible for Swedish familial AD backcrossed to C57BL/6 for 2 generations was mated with $TTR^{-/-}$ female mice backcrossed to C57BL/6 for eight generations (9). The $TTR^{+/-}$ F1 male mice carrying the mutant APP cDNA were mated with $TTR^{-/-}$ female mice. Heterozygous ($TTR^{+/-}$) F2 male mice carrying the mutant APP cDNA (Tg2576/$TTR^{+/-}$) were mated with $TTR^{-/-}$ F2 female mice. The $TTR^{+/-}$ and $TTR^{-/-}$ F3 progenies carrying the mutant APP cDNA (Tg2576/$TTR^{+/-}$ and Tg2576/$TTR^{-/-}$) were used in the present study. The F3 transgenic mice were maintained in cages housing three to six mice each, on separate racks in the same room, kept under a 12-h light cycle. Regular rodent's chow (Oriental Yeast, Tokyo, Japan) and tap water were freely available.

Transgenic mice were killed by cervical dislocation after anesthesia with diethyl ether. The brains were dissected; the right hemi-brains were immediately frozen in liquid nitrogen and stored at −80°C while the left hemi-brains were fixed in 4% buffered paraformaldehyde, and embedded in paraffin. Genotype analysis for each animal was carried out by polymerase chain reaction on DNA, purified from tails, as described (9, 14). The presence and absence of TTR in the serum of Tg2576/$TTR^{+/-}$, and Tg2576/$TTR^{-/-}$ mice, respectively, were confirmed by western blotting analysis as described (51).

All animal experiments were approved by University of Yamanashi Animal Care and Use Committee.

Immunohistochemistry

For brain Aβ detection, the paraffin-embedded left hemi-brain sections (5 μm) were pretreated with 99% formic acid for 3 minutes and immersed in 5% periodic acid for 10 minutes to block endogenous peroxidase. They were then incubated with blocking buffer [5% normal goat serum (Gibco, Carlsbad, CA, USA) in 10-mM phosphate buffer pH 7.4 and 100-mM NaCl with 0.05% Tween-20 (Bio-Rad, Richmond, CA, USA) containing Block Ace (Dainipponseiyaku, Suita, Japan)] for 1 h, with primary antibody [Ab9204 recognizing normal L-aspartate at position 1 (34), 0.1 μg/ml] overnight, and with biotinylated anti-rabbit immunoglobulin G (IgG) antibody (1:200) (Vector Laboratories, Burlingame, CA, USA) for 1 h. Immunoreactivity was visualized with the use of Vectastain ABC Elite kit (Vector Laboratories, Burlingame, CA, USA), and 3,3′-diaminobenzidine, tetrahydrocloride (DAB). Tissue sections were counterstained with hematoxylin.

For phosphorylated tau detection, the paraffin sections were pretreated with periodic acid, as described above and then irradiated in 10-mM citric acid buffer pH 6.0 for 15 minutes with microwave oven. After blocking, as described above, the sections were stained with the use of primary antibody AT8, recognizing phosphorylated tau at Ser202/Thr205 (1:500) (Innogenetics, Gent, Belgium) or anti-phosphorylated tau, recognizing phosphorylated tau at Thr231 (Thr231; 1:1000) (Calbiochem, Darmstadt, Germany), and Vectastain ABC Elite kit and counterstained by hematoxylin.

Fragmented DNA of apoptotic cells in the brain was detected by terminal deoxynucleotidyl transferase-mediated dUTP nick end labeling (TUNEL) method with the use of DeadEnd Colorimetric TUNEL System (Promega, Madison, WI, USA) and DAB according to the manufacturer's instructions.

Quantification of Aβ burden by image analysis

For quantification of Aβ burden, immuno-labeling was examined in the entire cerebral cortex and hippocampal areas of Tg2576/$TTR^{+/-}$ and Tg2576/$TTR^{-/-}$ mice. The amyloid burden was calculated by dividing total area of Aβ deposits by total area of region analyzed (in pixels). Images were captured and analyzed with the use of ImagePro®ver6 software (Media Cybernetics, Silver Spring, MD, USA). Four coronal sections from each of the mice were examined. The burden was expressed as mean ± standard error of the mean.

Protein extraction

Frozen right hemi-brains were sequentially extracted using two-step extraction method, as described previously (18). Initially, the frozen brain samples were homogenized in 2% sodium dodecylsulfate (SDS) (150 mg/ml wet weight) with protease inhibitors (complete protease inhibitor cocktail, one tablet in 50-ml solution; Boehringer Mannheim, Mannheim, Germany) followed by centrifugation at 100,000 ***g*** for 1 h at 4°C. The supernatant was then removed (termed SDS fraction), and the resultant pellet was sonicated [(35 s at level 10; XL-2000 Microson Ultrasonic Cell Disruptor (Misonix Inc., Farmingdale, NY, USA)] in 70% formic acid in water. After sonication, the samples were centrifuged, as described above, and the supernatant was removed (termed FA fraction). Total protein concentration measurement for SDS fraction was carried out with the use of BCA Kit (Pierce, Rockford, IL, USA).

Western blotting analysis

The SDS fractions of brain extracts (30 μg of protein) were electrophoresed on 4–12% gradient Bis-Tris gels (NuPage, Invitrogen, Carlsbad, CA, USA) and transferred to polyvinylidene difluoride membranes (Tefco, Tokyo, Japan). Membranes were labeled with the use of primary antibody, Saeko (1:1000), recognizing C terminal 30 amino acids of both human and mouse APP (18) overnight at 4°C, incubated with horseradish peroxidase-linked anti-rabbit IgG antibody (Amersham Biosciences, Buckingham, UK) (1:2000) for 1 h, and the immunoreactivity was visualized with the use of Supersignal (Pierce, Rockford, IL, USA). Images were captured by Fuji Bas-1000 imaging analyzer (Fujifilm, Tokyo, Japan), and the

intensity of the bands was quantified with the use of Scion Image (Scion Corp., Frederick, MD, USA).

Sandwich enzyme-linked immunosorbent assay

Amyloid-β 40 and Aβ42 in the brain extracts (SDS and FA fractions) were measured by sandwich enzyme-linked immunosorbent assay (ELISA), as described previously (18, 24, 25). Microplates (Immunoplate I, Nunc, Rockilde, Denmark) were pre-coated with anti-Aβ monoclonal antibody BNT77 (IgA isotype specific for Aβ11-16) that recognizes both Aβ40 and Aβ42, then incubated for 24 h at 4°C with 100 µl/well of samples. The microplates were further incubated for 24 h at 4°C with either horseradish-peroxidase-conjugated BA27 (anti-Aβ1-40, specific for Aβ40) or BC-05 (anti-Aβ35-43, specific for Aβ42 and Aβ43). Color was developed with 3,3′,5,5′-tetramethylbenzidine and evaluated at 450 nm on a microplate Reader (Molecular Devices, Menlo Park, CA, USA). The SDS fractions were diluted 400 times in EC buffer [20-mM phosphate buffer, pH 7.0, 400-mM NaCl, 2-mM EDTA, 0.4% Block Ace (Dainipponseiyaku, Suita, Japan), 0.2% bovine serum albumin, 0.05% CHAPS and 0.05% sodium azide] containing 0.005% SDS. The FA fraction was neutralized by a 1:50 dilution into 1-M Tris-HCl, pH 8.0 and then further diluted 20 times in EC buffer. The program Softmax (Molecular Devices, Menlo Park, CA, USA) was used to calculate Aβ concentration (in picomolar) by comparing the sample absorbance with the absorbance of known concentrations of synthetic Aβ42 or Aβ40 standards (Sigma, St Louis, MO, USA) assayed identically on the same plate. Using the wet weight of brain in the original homogenate, the final values of Aβ in brain were expressed as picomoles per gram wet weight.

Statistical analysis

The difference in the Aβ burden between Tg2576/*TTR*$^{+/-}$ and Tg2576/*TTR*$^{-/-}$ mice was examined with ANOVA followed by the Student's unpaired *t*-test with GraphPad Prism, Version 4.0 (GraphPad Software, San Diego, CA, USA). $P < 0.05$ was considered significant.

RESULTS

There is no significant difference in the brain levels of full-length APP between Tg2576/TTR$^{+/-}$ and Tg2576/TTR$^{-/-}$ mice

Amyloid-β peptides are derived from APP. To determine whether or not TTR affected the level of full-length APP, the groups of two Tg2576/*TTR*$^{+/-}$ and Tg2576/*TTR*$^{-/-}$ littermates were killed at 16, 18 and 20 months of age, and relative levels of full-length APP in the SDS fractions prepared from the brain were determined by western blotting with the use of Saeko, as described under *Methods*. Significant differences were never detected in the levels of full-length APP among any of the Tg2576/*TTR*$^{+/-}$ and Tg2576/*TTR*$^{-/-}$ mice examined (Figure 1). Thus, TTR does not affect the level of full-length APP in the brain of Tg2576 mice.

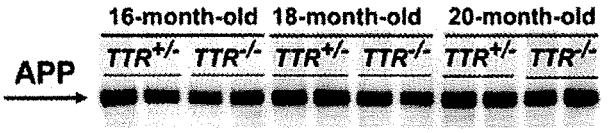

Figure 1. *Western blotting analysis of full-length amyloid precursor protein (APP).* The arrow on the left indicates the location of full-length APP.

Transthyretin deficiency does not increase but decreases the degree of total and vascular Aβ burdens in the brain of Tg2576 mice

Total Aβ burden

To evaluate whether or not TTR affected Aβ deposition, we compared the onset, progression and distribution of amyloid deposition between the brain of Tg2576/*TTR*$^{+/-}$ and Tg2576/*TTR*$^{-/-}$ mice, measuring the area occupied by Aβ deposits around the vascular wall of the meninx and cerebral parenchyma (termed cerebral amyloid angiopathy; CAA) and inside the brain parenchyma (termed Aβ plaque), as described under *Methods*. A time-course analysis of the total Aβ deposition in the brain was performed by assessing mice of ages 7–20 months. The number and age of mice examined were shown in Table 1. Aβ deposits were not detected in any of the six 7–11-month-old Tg2576/*TTR*$^{+/-}$ and Tg2576/*TTR*$^{-/-}$ mice examined. A small amount of Aβ deposits was first observed at 12 months of age in both the mice (data not shown). With advancing age, total Aβ burden increased (Figure 2A), and Aβ deposits were observed in the cerebral cortex, neocortex and hippocampus (Figure 3A), but not in the cerebellum (data not shown) in both the mice. Although there was a trend to reduction of total Aβ burden in 12–17-month-old Tg2576/*TTR*$^{-/-}$ mice relative to the age-matched Tg2576/*TTR*$^{+/-}$ mice, there was no statistically significant difference in the onset, progression and distribution of total Aβ deposition in the entire cerebral cortex between Tg2576/*TTR*$^{+/-}$ and Tg2576/*TTR*$^{-/-}$ mice (Figure 2A). The size of Aβ deposits in Tg2576/*TTR*$^{-/-}$ mice was also much the same as that in the age-matched Tg2576/*TTR*$^{+/-}$ mice. In 18–20-month-old Tg2576/*TTR*$^{-/-}$

Table 1. The number and age of mice examined by immunohistochemistry. Abbreviation: n = number of mice.

Age (months)	Tg2576/*TTR*$^{+/-}$ (n)	Tg2576/*TTR*$^{-/-}$ (n)
7	2	2
8	2	2
11	2	2
12	2	2
13	5	5
14	6	6
15	6	6
16	6	6
17	3	3
18	6	6
20	2	2
Total	42	42

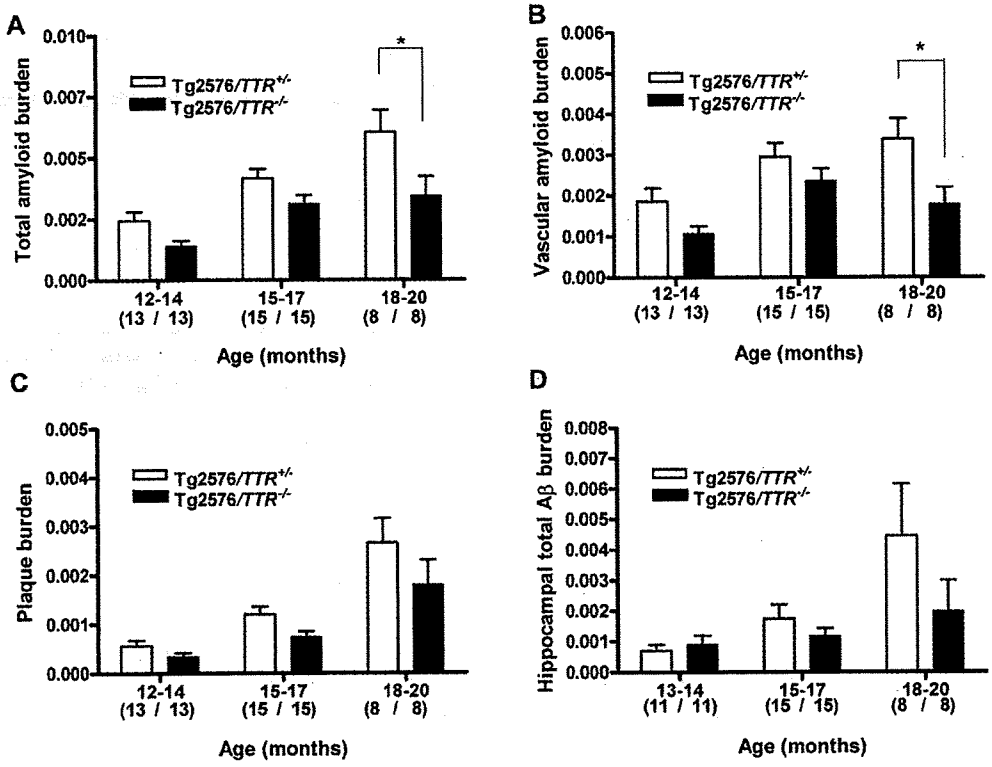

Figure 2. *The Aβ burden in the brain of Tg2576/TTR$^{+/-}$ and Tg2576/TTR$^{-/-}$ mice.* The total Aβ burden (vascular amyloid and plaques) (**A**) vascular Aβ burden (**B**) and Aβ plaque burden (**C**) in the entire cerebral cortex were calculated by dividing total area of Aβ deposits by total area of analyzed cortex. The hippocampal total Aβ burden (**D**) was calculated by dividing area of total Aβ deposits (vascular amyloid and plaques) by area of analyzed hippocampus. All data are expressed as mean ± standard error of the mean. Numbers in parentheses denote numbers of mice examined. *$P < 0.05$. TTR = transthyretin.

mice, however, total Aβ burden was significantly reduced relative to the age-matched Tg2576/*TTR*$^{+/-}$ mice ($P < 0.05$) (Figure 2A). Thus, contrary to our expectations, total Aβ burden is not increased, but rather decreased by eliminating TTR in Tg2576 mice.

Vascular Aβ burden

It had been reported that Tg2576 mice developed abundant vascular amyloid while aging, especially in leptomeningeal vessels (31). In order to determine whether the onset and degree of particular form of Aβ deposition were affected by TTR, we separately assessed vascular amyloid and plaque burdens in the brain of Tg2576/*TTR*$^{+/-}$ and Tg2576/*TTR*$^{-/-}$ mice, as described under *Methods*.

A time-course analysis of vascular Aβ burden was performed by assessing the mice of ages 7–20 months. A few vascular Aβ deposits were first observed at 12 months of age in both Tg2576/*TTR*$^{+/-}$ and Tg2576/*TTR*$^{-/-}$ mice. With advancing age, total vascular Aβ burden increased in both the mice (Figure 2B). Vascular Aβ deposits were detected only in the wall of leptomeningeal vessels of 12–16-month-old Tg2576/*TTR*$^{+/-}$ and Tg2576/*TTR*$^{-/-}$ mice, while in the 17–20-month-old Tg2576/*TTR*$^{+/-}$ and Tg2576/*TTR*$^{-/-}$ mice, the deposits were detected in the vascular wall of cerebral parenchyma as well as the wall of leptomeningeal vessels (data not shown). There was no significant difference in the onset, progression and distribution of vascular Aβ deposition in the entire cerebral cortex between Tg2576/*TTR*$^{+/-}$ and Tg2576/*TTR*$^{-/-}$ mice up to 17 months of age. However, a significant reduction in vascular Aβ burden by 47.1% was found in 18–20-month-old Tg2576/*TTR*$^{-/-}$ mice relative to the age-matched Tg2576/*TTR*$^{+/-}$ mice ($P < 0.05$) (Figure 2B). These findings suggested that TTR does not decrease but rather increases the degree of vascular Aβ burden in Tg2576 mice.

Amyloid-β plaque burden

Aβ plaques were first detected in both Tg2576/*TTR*$^{+/-}$ and Tg2576/*TTR*$^{-/-}$ mice at 12 months of age, and both the size and number of the plaques increased with advancing age (Figure 2C). Although there was a trend to reduction of total Aβ plaque burden in 12–20-month-old Tg2576/*TTR*$^{-/-}$ mice relative to the age-matched Tg2576/*TTR*$^{+/-}$ mice, there was no statistically significant difference in the onset, degree and distribution of Aβ plaque deposition between Tg2576/*TTR*$^{+/-}$ and Tg2576/*TTR*$^{-/-}$ mice (Figure 2C). These findings suggested that TTR does not decrease Aβ plaque burden in the brain of Tg2576 mice.

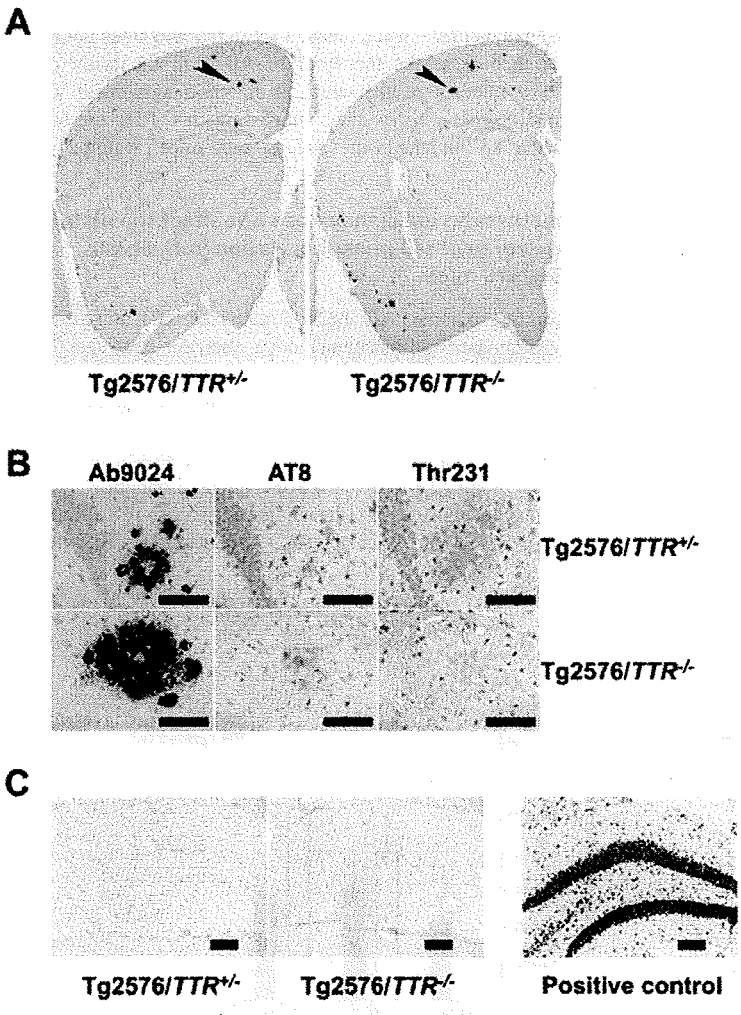

Figure 3. *Immunohistochemistry of Tg2576/TTR$^{+/-}$ and Tg2576/TTR$^{-/-}$ brains.* Immuno-labeling of left hemi-brain sections of 18-month-old Tg2576/*TTR*$^{+/-}$ and Tg2576/*TTR*$^{-/-}$ mice with Ab9204. **A**. The higher magnification of the hippocampal Aβ plaque with giant cores indicated by an arrowhead in **A** (**B**, *left panels*). Serial sections (5 μm) were labeled with AT8, and anti-phosphorylated tau (Thr231). AT8 and Thr-231 labeled punctate dystrophic neurites in and around Aβ plaques (**B**, *middle and right panels, respectively*). Scale bar; 50 μm. The hippocampal dentate gyrus areas of 18-month-old Tg2576/*TTR*$^{+/-}$ and Tg2576/*TTR*$^{-/-}$ mice stained with transferase-mediated dUTP nick end labeling. **C**. No apoptotic cells were found in the hippocampus. A DNaseI-treated sample was stained in parallel with the samples as a positive control. Scale bar; 100 μm. TTR = transthyretin.

Transthyretin deficiency does not affect Aβ deposition in the hippocampus of Tg2576 mice

The hippocampus is highly susceptible area to Aβ deposition in both humans (5) and Tg2576 mice (15). To investigate the effect of TTR deficiency on Aβ deposition in the hippocampus, we measured the total Aβ burden in the hippocampus of Tg2576/*TTR*$^{+/-}$ and Tg2576/*TTR*$^{-/-}$ mice. The Aβ deposits were first detected in the hippocampus of both the mice at 13 months of age, and showed an age-related increase (Figure 2D). Although the total Aβ burden in Tg2576/*TTR*$^{+/-}$ mice was consistently greater than that in Tg2576/*TTR*$^{-/-}$ mice, the difference was not statistically significant. Thus, the TTR deficiency does not affect Aβ deposition in the hippocampus of Tg2576 mice.

Transthyretin deficiency does not increase but decreases the level of Aβ40 in the brain of Tg2576 mice

Different forms of Aβ, biochemically distinguishable by their solubility properties, are present in varying amounts during the lifetime of Tg2576 mice. Detergent-soluble Aβ (SDS fraction) is present throughout life; however, detergent-insoluble Aβ (FA fraction) is absent up to age 6 months (18). It had been reported in AD that the predominant Aβ peptide present in CAA is Aβ40; however, in brain parenchymal plaques, it is Aβ42 (1, 7, 17, 29, 44). To evaluate whether or not TTR affects the level of different forms of Aβ, we quantified the Aβ40 and Aβ42 in SDS and FA fractions of brain homogenates from Tg2576/*TTR*$^{+/-}$ and Tg2576/*TTR*$^{-/-}$ mice by sandwich ELISA, as described under *Methods*. The number and age of 13–20-month-old Tg2576/*TTR*$^{+/-}$ and Tg2576/*TTR*$^{-/-}$ mice examined were shown in Table 2. Aβ40 and Aβ42 levels in SDS and FA fractions increased with age in both the mice. There was no significant difference in the levels of Aβ40 and Aβ42 in both the fractions between Tg2576/*TTR*$^{+/-}$ and Tg2576/*TTR*$^{-/-}$ mice up to 17 months of age. In 18–20-month-old Tg2576/*TTR*$^{-/-}$ mice, however, the levels of Aβ40 in both SDS and FA fractions were significantly reduced by 35.2% and by 41.6%, respectively, relative to the age-matched Tg2576/*TTR*$^{+/-}$ mice ($P < 0.05$) (Figure 4A,B). The level of Aβ42 in SDS fraction was also significantly reduced by 57.8% in 18–20-month-old

Table 2. The number and age of mice examined by sandwich enzyme-linked immunosorbent assay. Abbreviation: n = number of mice.

Age (months)	Tg2576/*TTR*$^{+/-}$ (n)	Tg2576/*TTR*$^{-/-}$ (n)
13	2	2
14	3	3
15	2	2
16	3	3
17	2	2
18	5	5
20	2	2
Total	19	19

Tg2576/*TTR*$^{-/-}$ mice relative to the age-matched Tg2576/*TTR*$^{+/-}$ mice ($P < 0.01$) (Figure 4C). On the other hand, there was no significant difference in the levels of Aβ42 in FA fraction between Tg2576/*TTR*$^{+/-}$ and Tg2576/*TTR*$^{-/-}$ mice (Figure 4D). The mean level of Aβ42 in FA fraction is much higher than that in SDS fraction. Thus, there was no significant difference in the sum of Aβ42 levels in both the fractions between aged Tg2576/*TTR*$^{+/-}$ and Tg2576/*TTR*$^{-/-}$ mice. Thus, TTR deficiency does not increase but rather decreases the level of Aβ40 in the brain of aged Tg2576 mice, a result, which is in good agreement with the immunohistochemistry data, suggesting that TTR increases the vascular Aβ burdens in the brain of aged mice (Figure 2).

Transthyretin deficiency does not affect the distribution and degree of tau phosphorylation in the brain of Tg2576 mice

In contrast to human AD, Tg2576 mice lack NFT, and develop the phosphorylated tau-immunoreactive aberrant structures that are exclusively associated with congophilic Aβ plaques (27, 48, 49). Stein *et al* reported that chronic infusion of an antibody against TTR into the hippocampus of Tg2576 led to an increase of tau phosphorylation within the CA1 neuronal field (42). To investigate whether or not TTR deficiency affected the distribution and degree of tau phosphorylation, the brain slices of 16–20-month-old Tg2576/*TTR*$^{+/-}$ and Tg2576/*TTR*$^{-/-}$ mice were stained with either

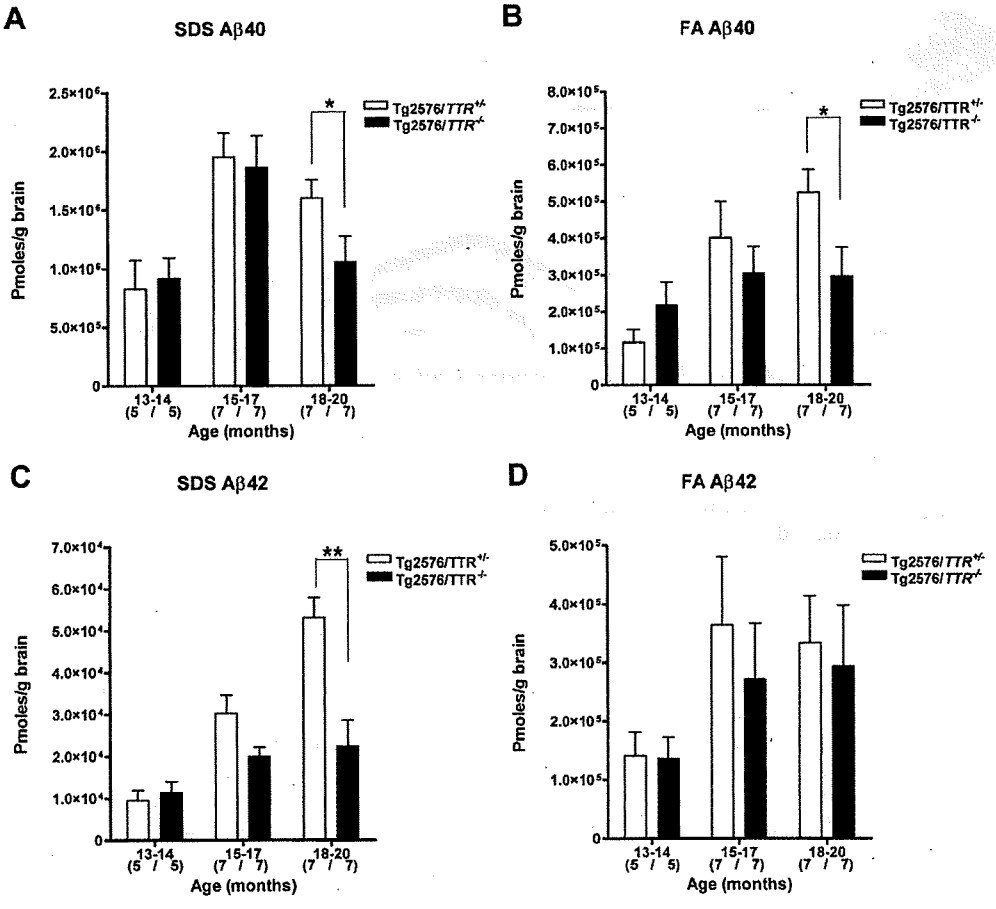

Figure 4. *The Aβ level in the brain of Tg2576/TTR*$^{+/-}$ *and Tg2576/TTR*$^{-/-}$ *mice.* The Aβ40 **(A,B)** and Aβ42 **(C,D)** in Tg2576/*TTR*$^{+/-}$ and Tg2576/*TTR*$^{-/-}$ brains were quantified by sandwich enzyme-linked immunosorbent assay. The samples were sequentially extracted in 2% sodium dodecylsulfate (SDS) **(A,C)** and 70% FA **(B,D)**. All data are expressed as mean ± standard error of the mean. Numbers in parentheses denote numbers of mice examined. $^{*}P < 0.05$, $^{**}P < 0.01$. TTR = transthyretin.

AT8 or Thr231 antibody, as described under *Methods*. Both the antibodies reacted only with the punctate dystrophic neurites (DNs) within the Aβ plaques in hippocampus and cerebral cortex in both the mice (Figure 3B). The abundance of the DNs immunopositive with the antibodies in Tg2576/*TTR*$^{-/-}$ mice was much the same as that in Tg2576/*TTR*$^{+/-}$ mice (Figure 3B). No NFT was detected in any of the mice examined. Thus, TTR deficiency does not affect tau phosphorylation in the brain of Tg2576 mice.

No apoptotic cells are detected in the hippocampus of Tg2576/TTR$^{+/-}$ and Tg2576/TTR$^{-/-}$ mice

Tg2576 mice do not develop severe neuronal loss observed in AD (15). Stein and Johnson suggested that high level of TTR in the hippocampus of Tg2576 mice might protect the mice from severe neuronal loss (43). Furthermore, the same group reported that chronic infusion of an antibody against TTR into the hippocampus of Tg2576 mice led to an increase of neuronal loss and apoptosis within the CA1 neuronal field (42). To determine whether or not TTR deficiency induces apoptosis in the hippocampus of Tg2576 mice, the brain sections from 18–20-month-old Tg2576/*TTR*$^{+/-}$ and Tg2576/*TTR*$^{-/-}$ mice were subjected to TUNEL immunohistochemistry, as described under *Methods*. Apoptotic cells were never detected in the hippocampus or other parts of brain of any of the mice examined (Figure 3C). These results indicate that TTR deficiency does not induce apoptosis in the brain of Tg2576 mice.

DISCUSSION

To investigate the role of TTR in the Aβ deposition *in vivo*, we generated a mouse line carrying a null mutation at the endogenous *TTR* locus and the human mutant APP cDNA with the Swedish mutation (Tg2576/*TTR*$^{-/-}$ mouse) by crossing Tg2576 mice with TTR-deficient mice generated through gene targeting. We then asked whether Aβ deposition was accelerated in Tg2576/*TTR*$^{-/-}$ mice relative to the heterozygous mutant Tg2576 (Tg2576/*TTR*$^{+/-}$) mice. Contrary to our expectations, the degree of total Aβ deposition, tau phosphorylation and apoptosis in the brain was not increased by eliminating TTR in Tg2576 mice. Moreover, the degree of vascular Aβ burden in the aged Tg2576/*TTR*$^{-/-}$ mice was significantly reduced relative to the age-matched Tg2576/*TTR*$^{+/-}$ mice. Our experiments present, for the first time, compelling evidence that TTR does not suppress but rather accelerates vascular Aβ deposition in the mouse model of AD.

We confirmed that there was no significant difference in the onset, progression and distribution of total Aβ deposition between Tg2576/*TTR*$^{+/-}$ and Tg2576/*TTR*$^{-/-}$ mice up to age 17 months by immunohistochemistry (Figure 2A). However, total Aβ burden in 18–20-month-old Tg2576/*TTR*$^{-/-}$ mice was significantly reduced relative to the age-matched Tg2576/*TTR*$^{+/-}$ mice ($P < 0.05$) (Figure 2A). The result suggested that TTR does not suppress but rather accelerates Aβ deposition in the brain of Tg2576 mice. Although both Tg2576/*TTR*$^{+/-}$ and Tg2576/*TTR*$^{-/-}$ mice are smaller than non-transgenic littermates, both of them display no obvious phenotypic abnormalities, and their fertility is normal up to age 10 months. This observation is consistent with the immunohistochemistry data.

We then separately assessed vascular amyloid and plaque burdens in the brain of Tg2576/*TTR*$^{+/-}$ and Tg2576/*TTR*$^{-/-}$ mice. Although Aβ plaque burden was much the same between 7–20-month-old Tg2576/*TTR*$^{+/-}$ and Tg2576/*TTR*$^{-/-}$ mice (Figure 2C), vascular amyloid burden in the aged (18–20-month-old) Tg2576/*TTR*$^{-/-}$ mice was significantly reduced relative to the age-matched Tg2576/*TTR*$^{+/-}$ mice ($P < 0.05$) (Figure 2B). The quantification of Aβ40 and Aβ42 in the brain homogenates from Tg2576/*TTR*$^{+/-}$ and Tg2576/*TTR*$^{-/-}$ mice by sandwich ELISA demonstrated that TTR deficiency does not increase, but rather decreases the level of Aβ40 in the aged Tg2576 mice (Figure 4). Because the predominant Aβ peptide present in vascular amyloid deposits is reportedly Aβ40 (1, 7, 44), the result is also in good agreement with our immunohistochemistry data (Figure 2), suggesting that TTR increases the vascular Aβ burden in the brain of aged Tg2576 mice.

The reason why vascular amyloid burden is increased by TTR is not clear. Amyloid deposits of all types, including Aβ deposits, contain glycosaminoglycans (GAGs) and serum amyloid P component (SAP). A role for GAGs in amyloidosis is inferred from the observation that small molecules that interfere with GAG/amyloid interactions reduce murine experimental amyloid A (AA) amyloid progression (19). An amyloid-binding protein SAP protects amyloid fibrils from proteolysis *in vitro* (46), and the induction of AA amyloidosis is significantly retarded in the SAP-deficient mice relative to wild-type mice (4, 47). On the other hand, recent evidence indicates that Aβ is mainly cleared out of the brain to blood via transport through the blood-brain barrier, and via the interstitial fluid (ISF) bulk flow along periarterial drainage pathways into the CSF, and from there into the blood (26, 33, 52, 56). It is the CSF and perhaps the ISF and not the brain parenchyma (41) that is enriched in TTR. Thus we think it likely that when Aβ drains from the brain parenchyma along periarterial drainage pathways, it may come into contact with TTR which may protect Aβ deposits from proteolysis like GAG and SAP, thereby, slightly increases vascular amyloid burden over the ages.

Schwarzman *et al* reported that TTR in the CSF binds Aβ, and prevents Aβ fibril formation *in vitro*. They, however, also reported that apoE prevents Aβ fibril formation too (36, 37). It has been well established that apoE promotes assembly of Aβ fibril (23, 32). Thus, TTR may promote the fibrillization of Aβ too. Moreover, Holtzman *et al* found that a transgenic mouse model of AD on an apoE$^{-/-}$ background had significantly reduced Aβ deposition relative to the same mouse model expressing wild-type murine apoE (apoE$^{+/+}$), human apoE3 (apoE3$^{+/-}$) or human apoE4 (apoE4$^{+/-}$) (12). Therefore, TTR null Tg2576 (Tg2576/*TTR*$^{-/-}$) mice may represent mice that are unable to form Aβ fibrils, and the Aβ detected in the brain of the mice could be due in part to apoE.

Stein *et al* reported that chronic infusion of anti-TTR antibody into the hippocampus of Tg2576 mice increased Aβ burden, and led to tau hyperphosphorylation, neuronal loss and apoptosis in the CA1 neuronal field (42). These observations suggest the importance of TTR in inhibition of Aβ fibril formation and toxicity. However, contrary to these reports, our experiments suggested that TTR does not suppress but rather enhances Aβ deposition in Tg2576 mice. The reason for the discrepancy between data of other authors and our data is not clear. TTR is complexed with retinol-binding protein (RBP) and thyroid hormone *in vivo*. In the *in vitro* Aβ aggregation assay, however, recombinant TTR alone, not complexed with RBP or thyroid hormone, was used to examine its ability to inhibit Aβ fibril formation (36, 37). Association of TTR with RBP and thyroid hormone may affect its binding capacity

with Aβ *in vivo*. Tau phosphorylation and apoptosis were induced by Aβ in hippocampal cultures (42). Thus, as suggested by Stein *et al*, high intrahippocampal concentration of Aβ, induced temporarily by the disruption of TTR binding of Aβ by the antibody, might have caused localized neurodegeneration in the CA1 field. The neurodegeneration reportedly detected in the antibody-infused limited area of hippocampus of Tg2576 mice (42), however, was not detected in the entire brain of TTR-deficient Tg2576 mice.

Stein and Johnson reported that the lack of neurodegeneration was associated with increased level of TTR synthesized in the hippocampus of Tg2576 mice (43). However, Lazarov *et al* reported that the individual levels of TTR mRNA in the hippocampi of a transgenic mouse model of AD, which co-expresses familial AD-linked mutant APP, and presenilin 1 (PS1) cDNAs were considerably variable (20). Furthermore, it had been reported that choroid plexus is the sole site of TTR synthesis within the brain; in this regard, Sousa *et al* recently confirmed that TTR is not produced in the brain parenchyma of either wild-type or Tg2576 mice, using laser dissection microscopy (41). The finding suggests that contamination by choroid plexus might lead to misinterpretation of the role of TTR in Aβ deposition in the brain.

In the present study, we compared the onset and progression of Aβ pathology in TTR null Tg2576 (Tg2576/$TTR^{-/-}$) mice with those in heterozygous mutant Tg2576 mice (Tg2576$TTR^{+/-}$). Thus, one factor which causes the discrepancy between our data and other authors' data obtained by examining only Tg2576 mice homozygous for the wild-type *TTR* gene (Tg2576/$TTR^{+/+}$) for comparison might be the difference in the levels of TTR. However, the onset and progression of Aβ pathology in our Tg2576/$TTR^{+/-}$ mice are rather delayed than accelerated relative to those in Tg2576/$TTR^{+/+}$ mice previously reported by other authors (6, 18, 45, 55). Thus, the possibility that homozygous levels of TTR would be required to prevent Aβ pathology appears to be remote.

On the other hand, Nunes *et al* reported that peptidylglycine α-amidating monooxygenase, the rate-limiting enzyme in neuropeptide maturation, is over-expressed in the peripheral, and central nervous systems of $TTR^{-/-}$ mice that, consequently, display increased neuropeptide Y (NPY) levels relative to wild-type mice (28). NPY is known to be a substrate of neprilysin, which is an Aβ-degrading protease (50). Another Aβ-degrading enzyme, insulin-degrading enzyme (IDE) is also known as insulin and amylin protease (30, 50). Hyperinsulinaemia is known to increase the risk of developing AD. Thus, it is suggested that hyperinsulinaemia may elevate Aβ level through insulin's competition with Aβ for IDE (30). Analogous to the competition, the increase in NPY levels in $TTR^{-/-}$ mice might competitively reduce neprilysin clearance of Aβ. Thus, Tg2576/$TTR^{-/-}$ mice might display enhanced Aβ deposition relative to Tg2576/$TTR^{+/-}$ mice through NPY's competition with Aβ for neprilysin. Contrary to the expectation, Tg2576/$TTR^{-/-}$ mice display rather suppressed Aβ deposition relative to Tg2576/$TTR^{+/-}$ mice (Figures 2 and 4). The results say that TTR does not suppress but rather accelerates Aβ deposition in Tg2576 mice.

Contrary to our findings, Choi *et al* recently reported that in a different transgenic mouse model of AD heterozygous for the disrupted *TTR* gene ($TTR^{+/-}$), brain Aβ deposition is significantly accelerated relative to the age-matched model homozygous for the wild-type *TTR* gene ($TTR^{+/+}$) (8). Their observation, which suggests that TTR suppresses Aβ deposition, contradicts ours. It is important to note that there are several critical differences in the experimental designs which might have caused the contradiction between their data and ours: (i) the AD model mouse we examined (Tg2576) is distinct from that Choi *et al* examined. They used *ceAPPswe/PS1ΔE9* mice that harbor not only the human mutant APP cDNA with the double mutation K670N and M671L linked to a Swedish familial AD but also the human mutant PS1 cDNA with the exon 9 deletion linked to a familial AD (16, 21). In contrast to Tg2576 mice, their control singly transgenic mice that express the human mutant APP cDNA alone are free of brain Aβ deposits up to age 14 months and co-expression of human mutant APP, and PS1 accelerates the amyloid deposition (3, 21). Furthermore, comparative analysis of cortical gene expression patterns between Tg2576 mice homozygous for the PS1 knock-in mutation (Tg2576/$PS1^{264L/264L}$) and control Tg2576 mice heterozygous for the PS1 mutation (Tg2576/$PS1P^{264L/+}$) by DNA micro-array analysis revealed that the patterns are distinct, although there were some common regulated genes (54). All these observations suggest that the molecular pathogenesis of Aβ deposition in the two mouse models is different; (ii) the level of human variant APP in the brain of Tg2576 mice is more than fourfold higher than that of endogenous brain APP (14). On the other hand, although the level of human variant APP in the brain of *ceAPPswe/PS1ΔE9* mice is not described (8), variant PS1ΔE9 reportedly elevates Aβ42/Aβ40 ratio (3). Thus the contradiction between their results and ours might be caused by the significant difference in the levels of Aβ42 and/or Aβ40 between Tg2576 and *ceAPPswe/PS1ΔE9* mice; and (iii) Choi *et al* compared the degree of Aβ deposition between the brains of *ceAPPswe/PS1ΔE9* mice heterozygous for the disrupted *TTR* gene ($TTR^{+/-}$) and the mice homozygous for the wild-type *TTR* gene ($TTR^{+/+}$) (8), in contrast to the TTR null ($TTR^{-/-}$) and $TTR^{+/-}$ Tg2576 mice we examined for comparison. Thus in their study, in contrast to our study, the individual differences in the levels of brain TTR among the $TTR^{+/-}$ and control $TTR^{+/+}$ mice should critically affect the results, and hence, the elucidation of the relationship between TTR and Aβ deposition. They described that the levels of immunoreactive TTR in the extracts from the brains of *ceAPPswe/PS1ΔE9/*$TTR^{+/-}$ mice are clearly lower relative to the age-matched *ceAPPswe/PS1ΔE9/*$TTR^{+/+}$ mice at all ages examined (8). However, the report is lacking in important details about the levels of TTR in the individual animals that would make the data more compelling. For example, given only the pictorial data with sample number of 1, it is not clear that the differences in the brain levels of TTR between *ceAPPswe/PS1ΔE9/*$TTR^{+/+}$ and *ceAPPswe/PS1ΔE9/*$TTR^{+/-}$ mice are really significant. On the other hand, it is possible that TTR, as a peripheral Aβ binding protein, may have the ability to act as a peripheral Aβ 'sink'; whereby, it pulls Aβ from the brain into the periphery, hence decreasing the amount of Aβ in the brain (26, 33, 52, 56). Thus, if we had examined Tg2576$TTR^{+/+}$ mice, we, too, might have detected a decrease in Aβ deposition as Choi *et al* did.

All the above differences may cause the contradiction between their data and ours. Moreover, they described that the levels of brain TTR were significantly lower in human AD patients compared with age-matched controls and negatively correlated with the abundance of amyloid plaques. However, the references they cited didn't refer to the brain TTR levels but to the CSF TTR levels in the patients (8) and, to our knowledge, the comparison of the brain TTR levels between AD patients and control disease-free individuals has not yet been reported.

In conclusion, our results indicated, for the first time, TTR does not suppress but accelerates vascular Aβ burden in the brain of Tg2576 mice. However, the mechanism(s) by which TTR affects the Aβ deposition *in vivo* are not yet elucidated. Taken together with the Choi et al's contradictory finding (8), our finding suggests that the role of TTR in the pathogenesis of AD remains to be understood.

ACKNOWLEDGMENTS

The authors would like to thank Drs. K. H. Ashe and Takaomi C. Saido for provision of Tg2576 mice and Ab9204 antibody, respectively. This work was supported by grants from the Ministry of Education, Culture, Sports, Science and Technology, Japan: Grants-in-aids for Scientific Research (18390098; to SM); and by grants to the Amyloidosis Research Committee for the Research on Intractable Diseases from the Ministry of Health, Labour and Welfare, Japan (to MS & SM).

REFERENCES

1. Alonzo NC, Hyman BT, Rebeck GW, Greenberg SM (1998) Progression of cerebral amyloid angiopathy: accumulation of amyloid-beta40 in affected vessels. *J Neuropathol Exp Neurol* **57**:353–359.
2. Biroccio A, Del Boccio P, Panella M, Bernardini S, Di Ilio C, Gambi D *et al* (2006) Differential post-translational modifications of transthyretin in Alzheimer's disease: a study of the cerebral spinal fluid. *Proteomics* 6:2305–2313.
3. Borchelt DR, Ratovitski T, van Lare J, Lee MK, Gonzales V, Jenkins NA *et al* (1997) Accelerated amyloid deposition in the brains of transgenic mice coexpressing mutant presenilin 1 and amyloid precursor proteins. *Neuron* **19**:939–945.
4. Botto M, Hawkins PN, Bickerstaff MC, Herbert J, Bygrave AE, McBride A *et al* (1997) Amyloid deposition is delayed in mice with targeted deletion of the serum amyloid P component gene. *Nat Med* **3**:855–859.
5. Braak H, Braak E (1991) Neuropathological stageing of Alzheimer-related changes. *Acta Neuropathol (Berl)* **82**: 239–259.
6. Carro E, Trejo JL, Gomez-Isla T, LeRoith D, Torres-Aleman I (2002) Serum insulin-like growth factor I regulates brain amyloid-beta levels. *Nat Med* **8**:1390–1397.
7. Castano EM, Prelli F, Soto C, Beavis R, Matsubara E, Shoji M, Frangione B (1996) The length of amyloid-beta in hereditary cerebral hemorrhage with amyloidosis, Dutch type. Implications for the role of amyloid-beta 1-42 in Alzheimer's disease. *J Biol Chem* **271**:32185–32191.
8. Choi SH, Leight SN, Lee VM, Li T, Wong PC, Johnson JA, Saraiva MJ, Sisodia SS (2007) Accelerated Abeta deposition in APPswe/PS1deltaE9 mice with hemizygous deletions of TTR (transthyretin). *J Neurosci* **27**:7006–7010.
9. Episkopou V, Maeda S, Nishiguchi S, Shimada K, Gaitanaris GA, Gottesman ME, Robertson EJ (1993) Disruption of the transthyretin gene results in mice with depressed levels of plasma retinol and thyroid hormone. *Proc Natl Acad Sci USA* **90**:2375–2379.
10. Giunta S, Valli MB, Galeazzi R, Fattoretti P, Corder EH, Galeazzi L (2005) Transthyretin inhibition of amyloid beta aggregation and toxicity. *Clin Biochem* **38**:1112–1119.
11. Hardy J, Selkoe DJ (2002) The amyloid hypothesis of Alzheimer's disease: progress and problems on the road to therapeutics. *Science* **297**:353–356.
12. Holtzman DM, Bales KR, Tenkova T, Fagan AM, Parsadanian M, Sartorius LJ *et al* (2000) Apolipoprotein E isoform-dependent amyloid deposition and neuritic degeneration in a mouse model of Alzheimer's disease. *Proc Natl Acad Sci USA* **97**:2892–2897.
13. Hsiao K, Chapman P, Nilsen S, Eckman C, Harigaya Y, Younkin S *et al* (1996) Correlative memory deficits, Abeta elevation, and amyloid plaques in transgenic mice. *Science* **274**:99–102.
14. Hsiao KK, Borchelt DR, Olson K, Johannsdottir R, Kitt C, Yunis W *et al* (1995) Age-related CNS disorder and early death in transgenic FVB/N mice overexpressing Alzheimer amyloid precursor proteins. *Neuron* **15**:1203–1218.
15. Irizarry MC, McNamara M, Fedorchak K, Hsiao K, Hyman BT (1997) APPSw transgenic mice develop age-related A beta deposits and neuropil abnormalities, but no neuronal loss in CA1. *J Neuropathol Exp Neurol* **56**:965–973.
16. Jankowsky JL, Slunt HH, Ratovitski T, Jenkins NA, Copeland NG, Borchelt DR (2001) Co-expression of multiple transgenes in mouse CNS: a comparison of strategies. *Biomol Eng* **17**:157–165.
17. Joachim CL, Duffy LK, Morris JH, Selkoe DJ (1988) Protein chemical and immunocytochemical studies of meningovascular beta-amyloid protein in Alzheimer's disease and normal aging. *Brain Res* **474**:100–111.
18. Kawarabayashi T, Younkin LH, Saido TC, Shoji M, Ashe KH, Younkin SG (2001) Age-dependent changes in brain, CSF, and plasma amyloid (beta) protein in the Tg2576 transgenic mouse model of Alzheimer's disease. *J Neurosci* **21**:372–381.
19. Kisilevsky R, Lemieux LJ, Fraser PE, Kong X, Hultin PG, Szarek WA (1995) Arresting amyloidosis in vivo using small-molecule anionic sulphonates or sulphates: implications for Alzheimer's disease. *Nat Med* **1**:143–148.
20. Lazarov O, Lee M, Peterson DA, Sisodia SS (2002) Evidence that synaptically released beta-amyloid accumulates as extracellular deposits in the hippocampus of transgenic mice. *J Neurosci* **22**:9785–9793.
21. Lazarov O, Robinson J, Tang YP, Hairston IS, Korade-Mirnics Z, Lee VM *et al* (2005) Environmental enrichment reduces Abeta levels and amyloid deposition in transgenic mice. *Cell* **120**:701–713.
22. Link CD (1995) Expression of human beta-amyloid peptide in transgenic Caenorhabditis elegans. *Proc Natl Acad Sci USA* **92**:9368–9372.
23. Ma J, Yee A, Brewer HB, Das S, Potter H (1994) Amyloid-associated proteins α_1-antichymotrypsin and apolipoprotein E promote assembly of Alzheimer β-protein into filaments. *Nature* **372**:92–94.
24. Matsubara E, Bryant-Thomas T, Pacheco Quinto J, Henry TL, Poeggeler B, Herbert D *et al* (2003) Melatonin increases survival and inhibits oxidative and amyloid pathology in a transgenic model of Alzheimer's disease. *J Neurochem* **85**:1101–1108.
25. Matsubara E, Ghiso J, Frangione B, Amari M, Tomidokoro Y, Ikeda Y *et al* (1999) Lipoprotein-free amyloidogenic peptides in plasma are elevated in patients with sporadic Alzheimer's disease and Down's syndrome. *Ann Neurol* **45**:537–541.
26. Matsuoka Y, Saito M, LaFrancois J, Saito M, Gaynor K, Olm V *et al* (2003) Novel therapeutic approach for the treatment of Alzheimer's disease by peripheral administration of agents with an affinity to beta-amyloid. *J Neurosci* **23**:29–33.
27. Noda-Saita K, Terai K, Iwai A, Tsukamoto M, Shitaka Y, Kawabata S *et al* (2004) Exclusive association and simultaneous appearance of congophilic plaques and AT8-positive dystrophic neurites in Tg2576 mice suggest a mechanism of senile plaque formation and progression of neuritic dystrophy in Alzheimer's disease. *Acta Neuropathol (Berl)* **108**:435–442.
28. Nunes AF, Saraiva MJ, Sousa MM (2006) Transthyretin knockouts are a new mouse model for increased neuropeptide Y. *Faseb J* **20**:166–168.

29. Prelli F, Castano E, Glenner GG, Frangione B (1988) Differences between vascular and plaque core amyloid in Alzheimer's disease. *J Neurochem* **51**:648–651.
30. Qiu WQ, Folstein MF (2006) Insulin, insulin-degrading enzyme and amyloid-beta peptide in Alzheimer's disease: review and hypothesis. *Neurobiol Aging* **27**:190–198.
31. Rensink AA, de Waal RM, Kremer B, Verbeek MM (2003) Pathogenesis of cerebral amyloid angiopathy. *Brain Res Brain Res Rev* **43**:207–223.
32. Sadowski MJ, Pankiewicz J, Scholtzova H, Mehta PD, Prelli F, Quartermain D, Wisniewski T (2006) Blocking the apolipoprotein E/amyloid-beta interaction as a potential therapeutic approach for Alzheimer's disease. *Proc Natl Acad Sci USA* **103**:18787–18792.
33. Sagare A, Deane R, Bell RD, Johnson B, Hamm K, Pendu R *et al* (2007) Clearance of amyloid-β by circulating lipoprotein receptors. *Nat Med* **13**:1029–1031.
34. Saido TC, Iwatsubo T, Mann DM, Shimada H, Ihara Y, Kawashima S (1995) Dominant and differential deposition of distinct beta-amyloid peptide species, a beta N3(pE), in senile plaques. *Neuron* **14**:457–466.
35. Sasaki A, Shoji M, Harigaya Y, Kawarabayashi T, Ikeda M, Naito M *et al* (2002) Amyloid cored plaques in Tg2576 transgenic mice are characterized by giant plaques, slightly activated microglia, and the lack of paired helical filament-typed, dystrophic neurites. *Virchows Arch* **441**:358–367.
36. Schwarzman AL, Goldgaber D (1996) Interaction of transthyretin with amyloid beta-protein: binding and inhibition of amyloid formation. *Ciba Found Symp* **199**:146–160.discussion 60–64.
37. Schwarzman AL, Gregori L, Vitek MP, Lyubski S, Strittmatter WJ, Enghilde JJ *et al* (1994) Transthyretin sequesters amyloid beta protein and prevents amyloid formation. *Proc Natl Acad Sci USA* **91**:8368–8372.
38. Serot JM, Christmann D, Dubost T, Couturier M (1997) Cerebrospinal fluid transthyretin: aging and late onset Alzheimer's disease. *J Neurol Neurosurg Psychiatry* **63**:506–508.
39. Seubert P, Vigo-Pelfrey C, Esch F, Lee M, Dovey H, Davis D *et al* (1992) Isolation and quantification of soluble Alzheimer's beta-peptide from biological fluids. *Nature* **359**:325–327.
40. Shoji M, Golde TE, Ghiso J, Cheung TT, Estus S, Shaffer LM *et al* (1992) Production of the Alzheimer amyloid beta protein by normal proteolytic processing. *Science* **258**:126–129.
41. Sousa JC, Cardoso I, Marques F, Saraiva MJ, Palha JA (2007) Transthyretin and Alzheimer's disease: where in the brain? *Neurobiol Aging* **28**:713–718.
42. Stein TD, Anders NJ, DeCarli C, Chan SL, Mattson MP, Johnson JA (2004) Neutralization of transthyretin reverses the neuroprotective effects of secreted amyloid precursor protein (APP) in APPSW mice resulting in tau phosphorylation and loss of hippocampal neurons: support for the amyloid hypothesis. *J Neurosci* **24**:7707–7717.
43. Stein TD, Johnson JA (2002) Lack of neurodegeneration in transgenic mice overexpressing mutant amyloid precursor protein is associated with increased levels of transthyretin and the activation of cell survival pathways. *J Neurosci* **22**:7380–7388.
44. Suzuki N, Iwatsubo T, Odaka A, Ishibashi Y, Kitada C, Ihara Y (1994) High tissue content of soluble beta 1-40 is linked to cerebral amyloid angiopathy. *Am J Pathol* **145**:452–460.
45. Takeuchi A, Irizarry MC, Duff K, Saido TC, Hsiao Ashe K, Hasegawa M *et al* (2000) Age-related amyloid beta deposition in transgenic mice overexpressing both Alzheimer mutant presenilin 1 and amyloid beta precursor protein Swedish mutant is not associated with global neuronal loss. *Am J Pathol* **157**:331–339.
46. Tennent GA, Lovat LB, Pepys MB (1995) Serum amyloid P component prevents proteolysis of the amyloid fibrils of Alzheimer disease and systemic amyloidosis. *Proc Natl Acad Sci USA* **92**:4299–4303.
47. Togashi S, Lim SK, Kawano H, Ito S, Ishihara T, Okada Y *et al* (1997) Serum amyloid P component enhances induction of murine amyloidosis. *Lab Invest* **77**:525–531.
48. Tomidokoro Y, Harigaya Y, Matsubara E, Ikeda M, Kawarabayashi T, Shirao T *et al* (2001) Brain Abeta amyloidosis in APPsw mice induces accumulation of presenilin-1 and tau. *J Pathol* **194**:500–506.
49. Tomidokoro Y, Ishiguro K, Harigaya Y, Matsubara E, Ikeda M, Park JM *et al* (2001) Abeta amyloidosis induces the initial stage of tau accumulation in APP (SW) mice. *Neurosci Lett* **299**:169–172.
50. Wang DS, Dickson DW, Malter JS (2006) beta-Amyloid degradation and Alzheimer's disease. *J Biomed Biotechnol* **2006**:58406.
51. Wei L, Kawano H, Fu X, Cui D, Ito S, Yamamura K *et al* (2004) Deposition of transthyretin amyloid is not accelerated by the same amyloid in vivo. *Amyloid* **11**:113–120.
52. Weller RO, Cohen NR, Nicoll JA (2004) Cerebrovascular disease and the pathophysiology of Alzheimer's disease. Implications for therapy. *Panminerva Med* **46**:239–251.
53. Westerman MA, Cooper-Blacketer D, Mariash A, Kotilinek L, Kawarabayashi T, Younkin LH *et al* (2002) The relationship between Abeta and memory in the Tg2576 mouse model of Alzheimer's disease. *J Neurosci* **22**:1858–1867.
54. Wu ZL, Ciallella JR, Flood DG, O'Kane TM, Bozyczko-Coyne D, Savage MJ (2006) Comparative analysis of cortical gene expression in mouse models of Alzheimer's disease. *Neurobiol Aging* **27**:377–386.
55. Yang F, Lim GP, Begum AN, Ubeda OJ, Simmons MR, Ambegaokar SS *et al* (2005) Curcumin inhibits formation of amyloid beta oligomers and fibrils, binds plaques, and reduces amyloid in vivo. *J Biol Chem* **280**:5892–5901.
56. Zlokovic BV (2004) Clearing amyloid through the blood-brain barrier. *J Neurochem* **89**:807–811.

特集2

認知症の克服に向けた創薬標的分子

Aβ分解酵素ネプリライシンによるアルツハイマー病の予防・治療戦略

斉藤貴志（さいとうたかし），岩田修永（いわたのぶひさ），津吹　聡（つぶきさとし），西道隆臣（さいどうたかおみ）
理化学研究所脳科学総合研究センター神経蛋白制御研究チーム
（〒351-0198 埼玉県和光市広沢2-1）
E-mail：takasai@brain.riken.jp　saido@brain.riken.jp

SUMMARY

アルツハイマー病（AD）は，神経機能障害～神経細胞死を原因とする認知症である．その原因は，脳内でアミロイドβペプチド（Aβ）および過剰リン酸化タウ（tau）の凝集・蓄積によって引き起こされると考えられている．現在，Aβの蓄積→tauの蓄積→神経細胞死という病理カスケード仮説（アミロイド仮説）に則った創薬研究が広く進められている．カスケードの上流と考えられる脳内Aβの蓄積は，認知機能障害を呈する遙か以前から始まっており，現在Aβの産生抑制・分解促進・凝集抑制法がADの予防・治療法のための創薬標的の一つとされている．我々はAβの分解を制御する機構に着目し，脳内でのAβ主要分解酵素であるネプリライシンを見出すに至った．本稿では，ネプリライシンの活性制御に基づくアルツハイマー病予防・治療への可能性について概説し，さらにAD脳に蓄積するAβが獲得する分解耐性機構についても取り上げ，新たな創薬標的として紹介したい．

KEY WORDS
アルツハイマー病（AD）
アミロイドβペプチド（Aβ）
ネプリライシン
ソマトスタチン（SST）
グルタミニルシクラーゼ（QC）

はじめに

現在の我が国において，認知症患者に対する介護のあり方がクローズアップされ身近な社会問題となっており，今後益々深刻化していく可能性が高い．これは，認知症，とりわけその大半を占めるアルツハイマー病（AD）に対する効果的な予防法・治療法が確立されていないことに一部端を発していると考えられる．我が国で唯一認められているAD治療薬には，塩酸ドネペジル（アリセプト）があるが，現状では未だ対症療法に留まっている．根治療法を可能にするための方法が世界中で模索されてはいるものの，未だに有効な方法に辿り着いていない．このような状況を打破するためにもADの発症メカニズムを解明し，そこに付随する新たな創薬標的を見出す必要がある．

AD予防・治療法の標的として重要視されているのは，AD患者の剖検脳で共通して見出される2大病理“老人斑”と“神経原線維変化”をそれぞれ構成するアミロイドβペプチド（Aβ）および，過剰リン酸化タウ（tau）の凝集・蓄積をいかに抑制するかという方法である．Aβの凝集・蓄積は神経細胞外（脳実質），tauの凝集・蓄積は神経細胞内で認められている．家族性ADの原因遺伝子が，Aβの前駆体タンパク質（APP）の遺伝子や，そのAPPからAβを産生す

1344-0128/10/¥100/頁/JCOPY

る際に関与するγセクレターゼ複合体のプレセニリン遺伝子から相次いで同定されている．このことは，Aβの蓄積がAD発症の引き金である可能性を示唆しており，アミロイド仮説として支持されている．Aβには40アミノ酸からなるAβ（1-40）と，さらに疎水性アミノ酸が2残基多くAβ（1-40）よりも遙かに神経毒性が高いAβ（1-42）の2種類が主として存在していることが知られている．また近年，C末端のアミノ酸残基が長い“longer Aβ”種や，逆に切断・修飾等を受けたAβ種も発見されており，それぞれがアミロイド病理形成に重要な役割を果たしていると考えられている．すなわち，Aβの代謝機構を解明することが，ADの予防・根本的治療法確立のための創薬標的を見出すために重要なのである．

I. Aβ分解とネプリライシン

全てのタンパク質は，産生と分解を繰り返す“代謝”というライフサイクルを持っている．この代謝制御が乱れた状態を「疾患」と捉えることができ，ADはまさにAβの代謝制御の乱れに端を発する疾患と考えられる（**図1a**）．上述したように，家族性ADの原因遺伝子はAβの産生に関与しており，その産生速度の増加を引き起こす．一方で，AD患者の大部分を占める孤発性AD（家族性は全体のわずか数%）の最大の危険因子は加齢であり，老化とは代謝機能の低下を伴うものである．孤発性ADではAβの産生増加はとくに認められていないことから，我々は，加齢に伴う

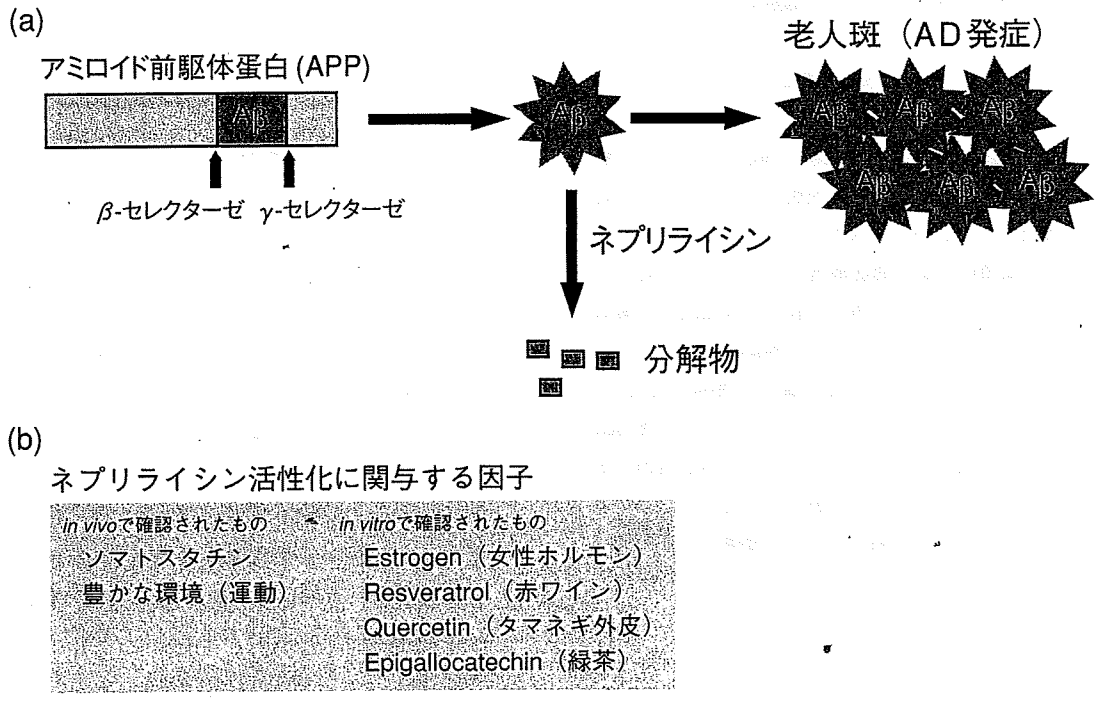

図1　Aβの産生・分解とネプリライシン活性制御因子

(a) Aβは，APPからβ，γ-セクレターゼの作用により産生され，ネプリライシンによって分解される．老化によるネプリライシン活性の低下により，分解を免れたAβは脳内で蓄積し始めプロトフィブリル形成を経由して，最終的には老人斑としてADの病理を呈する．(b) ネプリライシンの活性化に関与する因子．

Aβ分解能の低下が，孤発性ADの原因の一つではないか？と考え研究を行ってきた．その結果，中性エンドペプチダーゼであるネプリライシンが脳内でのAβ分解に寄与する主要なプロテアーゼであることを明らかにした[1]．これを機に，Aβ代謝における分解系の重要性が注目されるようになってきた．ネプリライシンは加齢に伴い発現が低下することや[2]，実際にAD脳でも活性・発現が低下していることからも[3]，ネプリライシン活性の低下がAβ分解能の低下，それに伴う脳内Aβレベルの増加に繋がると考えられ，孤発性ADの部分的な原因となる可能性が示唆されている．すなわち，脳内でネプリライシン活性を増強させることがADの予防・治療に効果がある可能性を示しており，実際，ネプリライシントランスジェニック（Tg）マウスとAPP Tgマウスの交配マウスを用いた解析[4]や，ネプリライシン遺伝子を組込んだアデノ随伴ウイルスをAPP Tgマウスの脳内に注入し，ネプリライシンの発現を高める方法[5]において，脳内Aβレベルの顕著な低下が認められている．

II. ネプリライシン活性制御因子ソマトスタチン

脳内ネプリライシン活性を高める方法がAβの分解・除去に有効であることから，ネプリライシンの活性制御機構を明らかにする必要性が提起された．そこで我々は，薬理学的に脳内ネプリライシンを活性化する方法を模索するため，ネプリライシン活性増強因子のスクリーニングを行った．その結果，神経ペプチドの一つであるソマトスタチン（SST）にネプリライシン活性増強作用があることが見出され，さらに，SST欠損マウスを用いた*in vivo*の解析により，SSTが脳内のネプリライシン活性制御因子であることを明らかにした[6]．SSTは，記憶力増強・安定化作用をはじめ多くの生理活性を持つ神経ペプチドであることが知られている．一方で，1980年代に，SSTがアセチルコリン同様にAD脳で低下している事が明らかとされていたが，その因果関係は長い間不明なままであった[7,8]．興味深いことに，SST欠損マウスの脳内では，Aβ（1-42）選択的な増加が認められ，その選択性は神経細胞におけるネプリライシンの局在が大きく関与している可能性が示唆された．SSTは，加齢に伴い脳内レベルが低下することも知られており[9]，これらの結果から我々は，「加齢に伴うSSTレベルの低下が脳内（特に海馬・歯状回）でのネプリライシン活性の低下を誘因し，その結果，Aβ（特にAβ（1-42））レベルを増加させ，最終的にADに至る」という仮説を提唱しており，孤発性ADの発症メカニズムを部分的に説明できるのではないかと考えている．このことは，SSTがADの予防・治療に有用である可能性だけでなく，加齢により脳内で低下したSSTを補う補充療法としての意味合いも併せ持つことを示している．

SSTは，ソマトスタチン受容体（SSTR）を介して生理作用を発揮していることが明らかとなっており，これまでに，5つのSSTRが同定されている．現在我々は，どのSSTRがネプリライシンの活性制御に関与しているか解析を進めている．これが明らかになれば，選択的なSSTR作動薬の開発に発展すると考えられる．

一方，ネプリライシン活性を抑制する因子もすでに同定しており，それに対する阻害物質も脳内のネプリライシン活性を保持する点で重要な創薬標的になりうると考えている．そのため，ネプリライシンの活性を制御する一連のメカニズムをより広く解明していくことが重要であると考えている．

III. ネプリライシン活性と環境因子

最近環境因子が様々な生理作用に影響を与えていることが明らかとなっている．ネプリライシンも同様で，豊かな環境（environmental enrichment）で飼育したAPP Tgマウスの脳内で，ネプリライシンの発現が選択的に増加していたという結果が報告されている[10]．さらに，豊かな環境で飼育したマウスの脳内でSSTの発現が増加しているという報告は，前述の実験結果を考えると非常に興味深い[11]．また，環境因子には，毎日の食事（食事成分）から受ける影響も含まれる．*In vitro*の解析ではあるが，赤ワインポリフェノールの一つresveratrol[12]やタマネギ外皮等の含有成分quercetin[12]，緑茶ポリフェノールの一つepigallocatechin[13]などにネプリライシン活性を増加する作用があると報告されて

いる．今後もこのような成分が見つかると予想され，生体内での効果の検証が待たれる．

また，疫学的には女性の方がADに罹りやすいという報告がある．様々な要因が考えられてはいるが，特に閉経後の女性ホルモン（エストロゲン）レベルの低下によるところが大きいと考えられている．最近，老齢ADモデルマウスでは，雌マウスにおいてネプリライシン活性が低下している事が報告された[14]．また，エストロゲン応答配列がネプリライシン遺伝子の上流に存在し，その発現を制御していることも報告された[15]．様々なストレスや環境ホルモン等の影響により性ホルモンのバランスに破綻をきたすことも知られており，多様な環境要因がネプリライシン活性に対し正にも負にも影響し，ADの発症に一部関与していることを示唆している（図1b）．このことは，毎日の食事や生活環境の改善を図ることで，ネプリライシンの活性化を含む身近なAD予防法に繋がる可能性を示している．

IV. Aβの分解耐性

これまでAβ分解機構に着目して多くの研究が進められてきたが，一方で，被分解基質としてのAβについても重要な報告が相次いでいる．AD発症に関連するAPP遺伝子変異の中でも，特に，図2に示すようなAβの内部配列に変異を持つ変異型Aβはネプリライシンに対して分解耐性を示し，生物学的半減期が長くなることが示された[16]．その結果，脳内Aβレベルが脳実質や脳血管で増加し，ADの発症に寄与すると推察されている．これらのことも，加齢に伴うネプリライシン活性の低下（Aβ分解能の低下）がADの発症に関与するという我々の仮説を補説しているだろう．

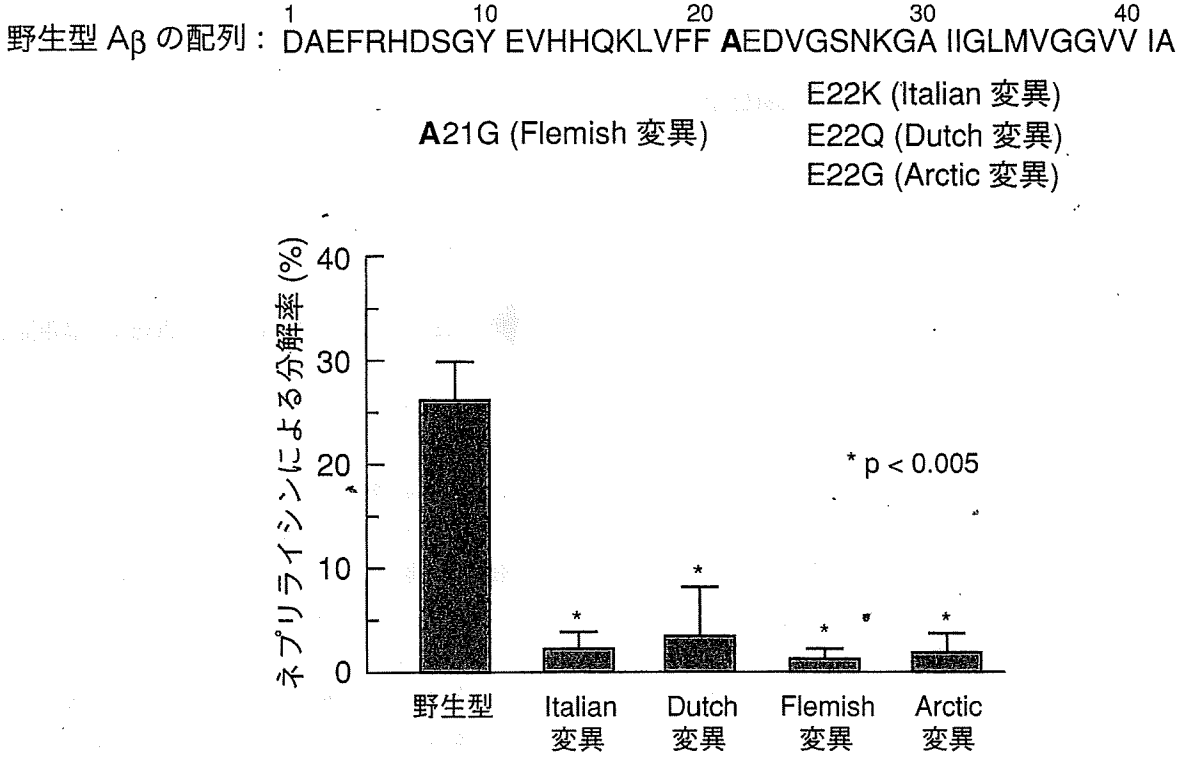

図2　Aβ内部配列変異が示すネプリライシン分解耐性

APP遺伝子のItalian, Dutch, Flemish, Arctic変異では，Aβの内部配列中に変異が存在している．これらの変異を持つAβは，ネプリライシンに対して分解耐性を獲得する[17]．

V. N3pE-Aβとグルタミニルシクラーゼ

AD患者の脳内ではAβのアミノ末端（N末端）が修飾を受けたもの，具体的には，3位のグルタミン酸がピログルタミル化したAβ（N3pE-Aβ）の存在比率が未修飾のAβと比較して大きいことが報告されている[17]．N3pE-AβはAβのN末端がアミノペプチダーゼやジペプチジルペプチダーゼ等のエキソペプチダーゼにより切断を受け，その後3位のグルタミン酸がグルタミニルシクラーゼ（glutaminyl cyclase：QC）の作用によりピログルタミル化したものである（図3）．N3pE-Aβは，Aβ（1-40）やAβ（1-42）よりもプロテアーゼに対する分解耐性が高く，生物学的半減期が長い．さらに，強い神経毒性を示すとともに，凝集能に至ってはAβ（1-42）の250倍も高いことが報告されている[18,19]．このことから，N3pE-Aβの産生はADの発症・進行を早める危険性があり，Aβのピログルタミル化を阻害し，プロテアーゼ耐性の獲得を阻害する方法も重要な創薬標的になるだろう．その標的となるQCは，亜鉛依存性のメタロエンザイムで，脳での発現も高いことが報告されている．最近QC阻害剤として開発されたイミダゾール誘導体PBD150が，N3pE-Aβの形成を*in vivo*でも抑制することが報告された[20]．このことは，Aβのピログルタミル化阻害とネプリライシン活性化を組み合わせた方法がより速やかにAβ分解・除去を促せると予想でき，QC阻害剤のさらなる検証が望まれている．

おわりに

Aβは認知症状が現れる20～30年前から脳内で蓄積している．このことは，ADを発症した時点では，病態はすでに進行した状況にあることを意味している．すなわち，ADの発症原因の一端を排除するためには，早期診断法の確立と予防法の確立が急務であるといえる．また，最近の報告では，ネプリライシンを高発現する血球系細胞を用いる方法[21]や，ミクログリ

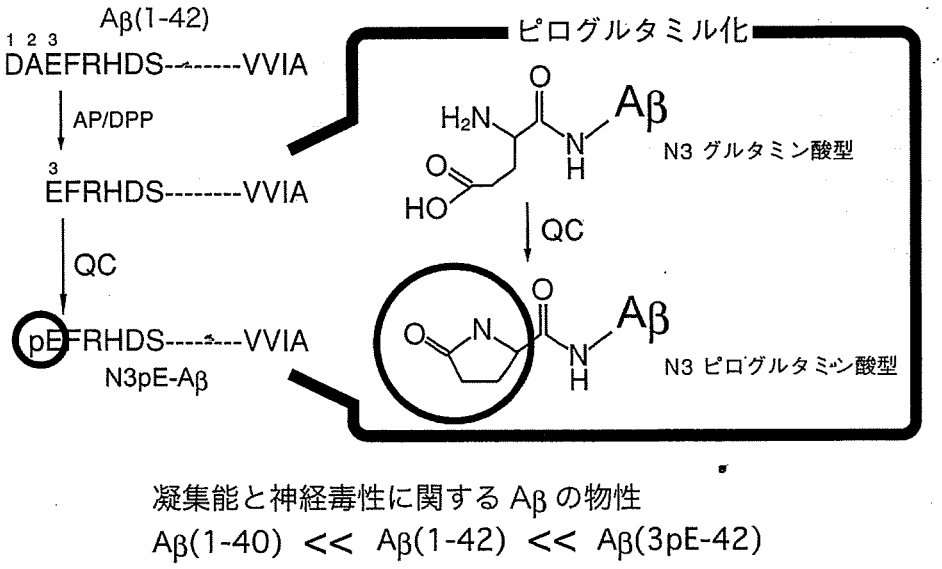

凝集能と神経毒性に関するAβの物性

Aβ(1-40) << Aβ(1-42) << Aβ(3pE-42)

図3　Aβのピログルタミル化

脳内で産生されたAβは，アミノペプチダーゼ（AP）やジペプチジルペプチダーゼ（DPP）のようなエキソペプチダーゼによって切断を受け，N末端3位のグルタミン酸（E）が露出する．このグルタミン酸がQCの作用によりピログルタミル化され，N3pE-Aβとなる．N3pE-Aβはプロテアーゼに対する分解耐性を持ち，強い神経毒性及び凝集性を示す．

ア[22]など非神経細胞でのネプリライシン活性の増強が脳内Aβ量に影響を及ぼす可能性を示唆しており，今後ネプリライシンを軸とした包括的なAD予防・治療法へ発展することが期待され，さらなる研究が進められている．

参考文献

1) Iwata N, et al : Metabolic regulation of brain Aβ by neprilysin. Science **292** : 1550-1552, 2001.
2) Hellstrom-Lindahl E, et al : Age-dependent decline of neprilysin in Alzheimer's disease and normal brain: Inverse correlation with Aβ levels. Neurobiol Aging **29** : 210-221, 2008.
3) Yasojima K, et al : Reduced neprilysin in high plaque areas of Alzheimer brain: a possible relationship to deficient degradation of β-amyloid peptide. Neurosci Lett **297** : 97-100, 2001.
4) Leissring MA, et al : Enhanced proteolysis of β-amyloid in APP transgenic mice prevents plaque formation, secondary pathology, and premature death. Neuron **40** : 1087-1093, 2003.
5) Iwata N, et al : Presynaptic localization of neprilysin contributes to efficient clearance of amyloid-β peptide in mouse brain. J Neurosci **24** : 991-998, 2004.
6) Saito T, et al : Somatostatin regulates brain amyloid β peptide Aβ42 through modulation of proteolytic degradation. Nature Med **11** : 434-439, 2005.
7) Davies P, et al : Reduced somatostatin-like immunoreactivity in cerebral cortex from cases of Alzheimer's disease and Alzheimer senile dementia. Nature **288** : 279-280, 1980.
8) Burgos-Ramos E, et al : Somatostatin and Alzheimer's disease. Mol Cell Endocrinol **286** : 104-111, 2008.
9) Lu T, et al : Gene regulation and DNA damage in the ageing human brain. Nature **429** : 883-891, 2004.
10) Lazarov O, et al : Environmental enrichment reduces levels and amyloid deposition in transgenic mice. Cell **120** : 701-713, 2005.
11) Nilsson L, et al : Environmental influence on somatostatin levels and gene-expression in the rat brain. Brain Res **628** : 93-98, 1993.
12) Melzig MF, Escher F : Induction of neutral endopeptidase and angiotensin-converting enzyme activity of SK-N-SH cells *in vitro* by quercetin and resveratrol. Pharmazie **57** : 556-558, 2002.
13) Ayoub S, Melzig MF : Induction of neutral endopeptidase (NEP) activity of SK-N-SH cells by natural compounds from green tea. J Pharm Pharmacoi **58** : 495-501, 2006.
14) Hirata-Fukae C, et al : Females exhibit more extensive amyloid, but not tau, pathology in an Alzheimer transgenic model. Brain Res **1216** : 92-103, 2008.
15) Liang K, et al : Estrogen stimulates degradation of β-amyloid peptide by upregulating neprilysin. J Biol Chem (in press).
16) Tsubuki S, et al : Dutch, Flemish, Italian, and Arctic mutations of APP and resistance of Aβ to proteolytic degradation. Lancet **361** : 1957-1958, 2003.
17) Saido TC, et al : Dominant and differential deposition of distinct β-amyloid peptide species, Aβ N3(pE), in senile plaques. Neuron **14** : 457-466, 1995.
18) Russo C, et al : The N- terminal pGlu could enhance the hydrophobicity, proteolytic stability and neurotoxicity of these peptides. J Neurochem **82** : 1480-1489, 2002.
19) Schilling S, et al : On the seeding and oligomerization of pGlu-amyloid peptides (*in vitro*). Biochemistry **45** : 12393-12399, 2006.
20) Schilling S, et al : Glutaminyl cyclase inhibition attenuates pyroglutamate Aβ and Alzheimer's disease-like pathology. Nature Med **14** : 1106-1111, 2008.
21) Guan H, et al : Peripherally expressed neprilysin reduces brain amyloid burden: A novel approach for treating Alzheimer's disease. J Neurosci Res **87** : 1462-1473, 2009.
22) Shimizu E, et al : IL-4-induced selective clearance of oligomeric β-amyloid peptide1-42 by rat primary type 2 microglia. J Immuno **181** : 6503-6513, 2008.

THE JOURNAL OF BIOLOGICAL CHEMISTRY VOL. 284, NO. 48, pp. 33400–33408, November 27, 2009

Depletion of Vitamin E Increases Amyloid β Accumulation by Decreasing Its Clearances from Brain and Blood in a Mouse Model of Alzheimer Disease*[S]

Received for publication, August 9, 2009 Published, JBC Papers in Press, August 13, 2009, DOI 10.1074/jbc.M109.054056

Yoichiro Nishida[‡], Shingo Ito[§], Sumio Ohtsuki[§], Naoki Yamamoto[¶], Tsubura Takahashi[‡], Nobuhisa Iwata[‖], Kou-ichi Jishage[**], Hiromi Yamada[‡], Hiroki Sasaguri[‡], Shigefumi Yokota[‡], Wenying Piao[‡], Hiroyuki Tomimitsu[‡], Takaomi C. Saido[‖], Katsuhiko Yanagisawa[¶], Tetsuya Terasaki[§], Hidehiro Mizusawa[‡], and Takanori Yokota[‡1]

From the [‡]Department of Neurology and Neurological Science, Graduate School, Tokyo Medical and Dental University, 1-5-45 Yushima, Bunkyo-ku, Tokyo 113-8519, the [§]Department of Molecular Biopharmacy and Genetics, Graduate School of Pharmaceutical Sciences, Tohoku University, Aoba, Aramaki, Aoba-ku, Sendai, Miyagi 980-8578, the [¶]National Institute for Longevity Sciences, National Center for Geriatrics and Gerontology, 36-3 Gengo, Morioka, Obu, Aichi 474-8522, the [‖]Laboratory for Proteolytic Neuroscience, RIKEN Brain Science Institute, 2-1 Hirosawa, Wako-shi, Saitama 351-0198, and the [**]Chugai Research Institute for Medical Science, Inc., Gotenba, Shizuoka 412-8513, Japan

Increased oxidative damage is a prominent and early feature in Alzheimer disease. We previously crossed Alzheimer disease transgenic (*APPsw*) model mice with α-tocopherol transfer protein knock-out (*Ttpa*$^{-/-}$) mice in which lipid peroxidation in the brain was significantly increased. The resulting double-mutant (*Ttpa*$^{-/-}$*APPsw*) mice showed increased amyloid β (Aβ) deposits in the brain, which was ameliorated with α-tocopherol supplementation. To investigate the mechanism of the increased Aβ accumulation, we here studied generation, degradation, aggregation, and efflux of Aβ in the mice. The clearance of intracerebral-microinjected ^{125}I-Aβ$_{1-40}$ from brain was decreased in *Ttpa*$^{-/-}$ mice to be compared with wild-type mice, whereas the generation of Aβ was not increased in *Ttpa*$^{-/-}$*APPsw* mice. The activity of an Aβ-degrading enzyme, neprilysin, did not decrease, but the expression level of insulin-degrading enzyme was markedly decreased in *Ttpa*$^{-/-}$ mouse brain. In contrast, Aβ aggregation was accelerated in *Ttpa*$^{-/-}$ mouse brains compared with wild-type brains, and well known molecules involved in Aβ transport from brain to blood, low density lipoprotein receptor-related protein-1 (LRP-1) and p-glycoprotein, were up-regulated in the small vascular fraction of *Ttpa*$^{-/-}$ mouse brains. Moreover, the disappearance of intravenously administered ^{125}I-Aβ$_{1-40}$ was decreased in *Ttpa*$^{-/-}$ mice with reduced translocation of LRP-1 in the hepatocytes. These results suggest that lipid peroxidation due to depletion of α-tocopherol impairs Aβ clearances from the brain and from the blood, possibly causing increased Aβ accumulation in *Ttpa*$^{-/-}$*APPsw* mouse brain and plasma.

The accumulation of amyloid β (Aβ)[2] is the primary pathological event driving neurodegeneration in Alzheimer disease (AD). Support of this hypothesis is based on genetic evidence from cases of familial AD with β-amyloid precursor protein (APP) or presenilin mutations and the remarkable effect of Aβ elimination by its vaccine on AD phenotype. The suggested mechanism for Aβ accumulation in sporadic AD includes elevated generation of Aβ due to increased β-secretase activity (1), decreased degradation of Aβ (2), and decreased efflux of Aβ from the brain to blood (3).

Increased oxidative stress of brain is a key feature of sporadic AD and manifests predominantly as lipid peroxidation (4). There are several lines of evidence suggesting that the AD brain displays extensive oxidative damage to various biological macromolecules, including lipids, proteins, and nucleic acids (5). Both Aβ level and lipid peroxidation in the brain are increased with disease progression of AD. However, the direct relationship between Aβ accumulation and lipid peroxidation is unclear (6).

Among natural isomers of vitamin E, α-tocopherol (α-Toc) has the most potent biological activity and is a major antioxidant that protects polyunsaturated fatty acids from peroxidation. Brain α-Toc content is maintained by α-tocopherol transfer protein (α-TTP), which transfers α-Toc from chylomicron to very low-density lipoprotein in the liver and transports α-Toc from blood to brain (7, 8). We have developed an α-tocopherol transfer protein knock-out (*Ttpa*$^{-/-}$) mouse that showed marked lipid peroxidation because of a lack of α-Toc in the brain and considered it as a model for chronic oxidative stress to the brain (7). In a *Ttpa*$^{-/-}$ mouse brain, two lipid peroxidation markers, thiobarbituric acid reactive substrates

* This work was supported in part by a grant for Research on Psychiatric and Neurological Disease and Mental Health from the Ministry of Health, Labor, and Welfare of Japan (to T. Y. and H. M.), a grant from the 21st Century COE Program on Brain Integration and Its Disorders to Tokyo Medical and Dental University (to Y. N., H. S., and H. M.), a grant from the Ministry of Education, Science, and Culture (to N. I., H. T., T. Y., and H. T.), and a grant of the SORST of Japan Science and Technology Agency (to S. O. and T. Terasaki).

[S] The on-line version of this article (available at http://www.jbc.org) contains supplemental Tables 1–3.

[1] To whom correspondence should be addressed. Tel.: 81-3-5803-5234; Fax: 81-3-5803-0169; E-mail: tak-yokota.nuro@tmd.ac.jp.

[2] The abbreviations used are: Aβ, amyloid β; AD, Alzheimer disease; APP, β-amyloid precursor protein; α-TTP, α-tocopherol transfer protein; PBS, phosphate-buffered saline; BBB, blood-brain barrier; LRP-1, lipoprotein receptor-related protein-1; Pgp, p-glycoprotein; GLUT-1, glucose transporter-1; TTR, transthyretin; BEI, brain efflux index; CLtot, total body clearance; α-Toc, α-tocopherol; TBS, Tris-buffered saline; PIPES, 1,4-piperazinediethanesulfonic acid; CHAPS, 3-[(3-cholamidopropyl)dimethylammonio]-1-propanesulfonic acid; IDE, insulin-degrading enzyme.

and 4-hydroxynonenal, were increased, and lipofuscin was massively accumulated (7). It is of note that the same markers were elevated in AD brains (9–11). We previously crossed the AD transgenic (*APPsw*) model mouse (Tg2576) with *Ttpa*$^{-/-}$ mouse, and the resulting double-mutant (*Ttpa*$^{-/-}$*APPsw*) mouse showed earlier and more severe cognitive dysfunction and had increased amyloid plaques in the brain by depletion of α-Toc (12). As a next step, we have studied the mechanism of how chronic lipid peroxidation increased Aβ deposits. The studies of the lifecycle of Aβ from its generation to its metabolism have received an extraordinary amount of attention in the field of AD research. Although the Aβ level in the brain is determined by the rate of Aβ generation and clearance in the brain, the clearance of Aβ from circulation is also important for the Aβ accumulation in the brain, because the Aβ levels in the brain and in the blood are held in equilibrium (3). Therefore, we evaluated the Aβ generation in the brain and its clearance from the brain and from the blood in *Ttpa*$^{-/-}$ mouse. We also measured the aggregation capacity of Aβ in the brain to evaluate the effect of oxidative stress on the accumulation of Aβ in the brain.

EXPERIMENTAL PROCEDURES

Animals

All experiments were approved by the Animal Experiment Committees of Tokyo Medical and Dental University. We used *Ttpa*$^{-/-}$ mice from a C57BL/6J background (7). We crossbred *Ttpa*$^{-/-}$ mice with *APPsw* transgene hemizygous mice (Tg2576 from a C57BL/6-SJL background, Taconic, Hudson, NY), which is an AD model that overexpresses a human APP_{695} with a double mutation (*APPsw*; K670N,M671L) (13). We then cross-bred *Ttpa*$^{+/-}$*APPsw* and *Ttpa*$^{+/-}$ to produce the *Ttpa*$^{-/-}$*APPsw* mice. Animals were screened for the presence of APPsw and α-TTP genes by PCR analysis of tail DNA. Complete elimination of α-Toc from the brain is achieved only when the deletion of α-TTP gene is combined with the dietary restriction, because a part of α-Toc taken up from the small intestine can enter the brain even without α-TTP (7). Furthermore, it is impossible to produce mice with α-Toc-deficient diet because supplementation of α-Toc is necessary for the maintenance of pregnancy (7). The dietary restriction of α-Toc after birth could not eliminate α-Toc from the brain of wild-type mice (7). Therefore, to study the effect of α-Toc depletion on AD phenotype, we fed the resulting double mutant (*Ttpa*$^{-/-}$*APPsw*) mice on α-Toc-deficient diet (Funabashi Farm, Chiba, Japan) and compared with the *APPsw* littermate mice on normal diet (36 mg of α-Toc/kg). To determine whether the differences in the phenotypes between *APPsw* mice and *Ttpa*$^{-/-}$*APPsw* mice are caused by the *Ttpa*$^{-/-}$ gene effect or α-Toc-deficient effect, we furthermore made a group of *Ttpa*$^{-/-}$*APPsw* mice that were fed on α-Toc-supplemented diet (750 mg of α-Toc/kg, Funabashi Farm). Details for these diets were previously described (7). All mice were housed in plastic cages, received food and water *ad libitum*, and were maintained on a 12/12-h light-dark cycle (lights on at 09:00, off at 21:00).

Aβ Quantitation in the Brain and Plasma

Three or four 18-month-old mice for each group were anesthetized with an intraperitoneal injection of pentobarbital (60 mg/kg). After blood was collected, they killed by transcardiac perfusion with 0.01 M phosphate-buffered saline (PBS), pH 7.4. The cerebral hemisphere was homogenized in 50 mM Tris-HCl buffer (TBS), pH 7.6, containing 150 mM NaCl and a protease inhibitor mixture (Complete, Roche Diagnostics) supplemented with 0.7 μg/ml pepstatin A (Peptide Institute, Osaka, Japan) with a Teflon glass homogenizer and centrifuged at 200,000 × *g* for 20 min at 4 °C. The supernatant was defined as the TBS-soluble fraction. The pellet was solubilized by sonication in 6 M guanidine-HCl buffer containing a protease inhibitor mixture. The solubilized pellet was centrifuged as before, after which the supernatant was diluted 12-fold to reduce the concentration of guanidine-HCl and used as the TBS-insoluble fraction (guanidine-extractable). The amounts of $Aβ_{1-40}$ and $Aβ_{1-42}$ in each fraction and plasma were assayed using commercially available human $Aβ_{1-40}$ and $Aβ_{1-42}$ sandwich enzyme-linked immunosorbent assay kits (BioSource International, Inc., Camarillo, CA).

Northern Blot Analysis

Three or four 18-month-old mice in each group were examined. Total RNA was extracted from the brain by TRIzol (Invitrogen). Total RNA (2.5 μg) was fractionated in a formaldehyde-agarose gel and transferred to a Nytran membrane (Schleicher & Schuell). The upper part of the membrane was hybridized with a purified PCR fragment corresponding to human APPsw cDNA (bases 981–1578). The lower part was hybridized with a probe specific for glyceraldehyde-3-phosphate dehydrogenase to confirm the quantity of loaded RNA. The signals were visualized with a Gene Images CDP-star detection kit (Amersham Biosciences).

Western Blot Analysis

C-terminal Fragments of APP-β, -α, and -γ/ε—Three or four 18-month-old mice in each group were examined. To analyze C-terminal fragments -β, -α, and -γ/ε, the cerebral hemisphere was homogenized with 50 mM TBS and centrifuged at 800 × *g* for 10 min at 4 °C. The supernatant was centrifuged at 200,000 × *g* for 28 min at 4 °C, and the resultant pellet was resuspended with 20 mM PIPES, pH 7.0, containing 140 mM KCl, 0.25 M sucrose, 5 mM EGTA, and a protease inhibitor mixture. Protein concentration was determined using a BCA protein assay kit (Pierce) and adjusted. After incubation of the suspension at 37 °C for 60 min, it was delipidized with chloroform: methanol (2:1) and chloroform:methanol:distilled water (1:2:0.8) sequentially to improve sensitivity. The resultant protein fraction was dried by evaporation and then solubilized with a sample buffer containing 9 M urea. Samples (20 μg) were separated by 16.5% SDS-polyacrylamide gel electrophoresis and transferred electrophoretically to nitrocellulose membranes (Schleicher & Schuell). The membranes were boiled in PBS for 3 min to improve sensitivity. The blot was probed with the rabbit polyclonal antibody against the C terminus of APP (A8717, Sigma) followed by the avidin-biotin-peroxidase complex (ABC) method (Vectastain ABC kits, Vector Laboratories,

Burlingame, CA). The immunoreactive band on the membrane was visualized with a Supersignal West Pico Chemiluminescence kit (Pierce).

Proteins to Transport Aβ across the Blood-Brain Barrier (BBB)—Three sets of three 8-month-old mice in each group were examined. The vascular fraction of small vessels was prepared from whole cerebrum using a modified method reported previously (14). Briefly, brains were homogenized in 10 mM PBS. After centrifugation at 800 × *g* for 5 min at 4 °C, the pellets were suspended with a dextran solution (M_r 70,000; 15% w/v, Sigma) and centrifuged at 4500 × *g* for 10 min at 4 °C. The pellets were washed by 10 mM PBS twice and resuspended with 5 mM PBS for 10 min. After centrifuging at 800 × *g* for 5 min, the final pellets of small vessels were resuspended by pipetting and vortexed in the homogenization buffer containing 10 mM TBS, pH 7.4, containing 1 mM EDTA, 150 mM NaCl, 4% CHAPS, 1 mM phenylmethylsulfonyl fluoride, and a protease-inhibitor mixture (Complete-Mini, Roche Diagnostics). The 4.5-μg samples were separated by 7.5 and 15% SDS-polyacrylamide mini-gel and transferred to a nitrocellulose membrane. The membrane was probed with mouse anti-low density lipoprotein receptor-related protein-1 (LRP-1) (β-chain specific, American Diagnostica Inc., Stamford, CT) or mouse anti-p-glycoprotein (Pgp) (C219, Signet, Dedham, MA) followed by sheep anti-mouse secondary antibody conjugated to horseradish peroxidase (Amersham Biosciences). Rabbit anti-brain-type glucose transporter-1 (GLUT-1) antibody (Alpha Diagnostic International, San Antonio, TX) with donkey anti-rabbit secondary antibody (Amersham Biosciences) was also used. Bands were visualized by using an ECL Plus Western blotting system (Amersham Biosciences).

Protein to Transport Aβ into the Liver—Three 8-month-old mice in each group were examined. To prepare the crude membrane fraction, liver was homogenized in hypotonic lysis buffer (10 mM Tris, 10 mM NaCl, 1.5 mM $MgCl_2$, pH 7.4) with 1 mM phenylmethylsulfonyl fluoride and a protease-inhibitor mixture (Complete-Mini). After centrifugation at 8000 × *g* for 10 min at 4 °C, the supernatant was centrifuged at 100,000 × *g* for 60 min at 4 °C. The pellet obtained was regarded as the crude membrane fraction. Furthermore, to prepare the plasma membrane fraction of the liver, this obtained pellet was resuspended in 10 mM HEPES, 250 mM sucrose, pH 7.4, and overlaid on 38% sucrose solution and then centrifuged at 100,000 × *g* for 40 min at 4 °C using a swing rotor (SW40Ti; Beckman, Fullerton, CA). The turbid layer was collected and centrifuged at 100,000 × *g* for 1 h at 4 °C, and the obtained pellet was defined as plasma membrane fraction. The 2.5-μg samples were separated with 7.5% SDS-polyacrylamide mini-gel and transferred electrophoretically to a nitrocellulose membrane. The membrane was probed with mouse anti-LRP-1, rabbit anti-cadherin (ab16505, Abcam, Cambridge, UK), or mouse anti-β-actin (A2228, Sigma) followed by sheep anti-mouse secondary antibody conjugated to horseradish peroxidase or a goat anti-rabbit antibody (Pierce), respectively. Bands were visualized by using an ECL Plus Western blotting system or a Supersignal West Femto Maximum Sensitivity kit (Pierce).

Aβ Ligand Proteins in the Plasma—Three or four 14-month-old mice in each group were examined. The collected plasma was diluted with saline, and the 0.10-μl anti-apolipoprotein E (apoE) or 0.40-μl anti-transthyretin (TTR) samples were separated with 15% SDS-polyacrylamide mini-gel and transferred electrophoretically to a polyvinylidene difluoride membrane (Bio-Rad). The membrane was probed with goat polyclonal anti-apoE (sc-6384, Santa Cruz Biotechnology, Inc., Santa Cruz, CA) or rabbit anti-TTR (Dako, Glostrup, Denmark) followed by donkey anti-goat secondary antibody conjugated to horseradish peroxidase (Santa Cruz Biotechnology) or donkey anti-rabbit antibody (Amersham Biosciences). Bands were visualized by using an ECL Plus Western blotting system.

Aβ Degrading Proteins in the Brain—Three or five 23-month-old mice in each group were examined. The cerebral hemisphere was homogenized in homogenization buffer (0.1 M Tris-HCl, pH 8.0, 0.15 M NaCl, 1 mg/ml leupeptin, and 1 mg/ml pepstatin A) and centrifuged at 500 × *g* for 5 min. Membranes were prepared by precipitation of the postnuclear supernatant at 100,000 × *g* for 60 min. The resulting pellet was subjected to protein extraction using 2% SDS by homogenization and posterior centrifugation at 100,000 × *g* for 60 min at 4 °C. The supernatant was used as a membrane fraction. Protein concentration was determined using a BCA protein assay kit, and the membrane fraction (2.5 μg) was separated by 7.5% SDS-polyacrylamide gel electrophoresis and transferred electrophoretically to polyvinylidene difluoride membrane. The blotted membrane was probed with rabbit polyclonal anti-insulin-degrading enzyme (IDE) (Calbiochem) or mouse anti-flotillin (BD Biosciences) followed by donkey anti-rabbit or sheep anti-mouse secondary antibody conjugated to horseradish peroxidase (Amersham Biosciences). Bands were visualized by using an ECL Plus Western blotting system.

β- and γ-Secretase Activities Measurement

The total activities of β- and γ-secretase present in the cerebrum of four 9-month-old mice were determined using secretase-kits (R&D Systems, Wiesbaden, Germany) (15). Secretase enzymatic activities were proportional to the fluorometric reaction, and the data were corrected by subtraction of background control (reactions in the absence of tissue).

Study of Aβ Efflux from the Brain at the BBB

In vivo brain elimination experiments were performed using intracerebral microinjection as described previously (16, 17). Four 2- or 14-month-old mice in each group were anesthetized intramuscularly with a mixture of ketamine (125 mg/kg) and xylazine (1.22 mg/kg), then mounted on a stereotaxic frame (SRS-6, Narishige, Tokyo, Japan) to hold the heads in position. Using a dental drill, a bore hole was made 3.8 mm lateral to the bregma. Then extracellular fluid buffer (122 mM NaCl, 25 mM $NaHCO_3$, 3 mM KCl, 1.4 mM $CaCl_2$, 1.2 mM $MgSO_4$, 0.4 mM K_2HPO_4, 10 mM D-glucose, and 10 mM HEPES, pH 7.4) containing 0.012 μCi of ^{125}I-Aβ_{1-40} and 0.12 μCi of [^{3}H]dextran was injected over a period of 1 min using a 5.0-μl microsyringe (Hamilton, Reno, NE) fitted with a fine needle at a depth of 2.5 mm from the surface of the scalp, *i.e.* in the secondary somatosensory cortex 2 (S2) region. The needle was left in this configuration for an additional 4 min to prevent reflux of the injected solution along the injection track before being slowly retracted.

At the designated times after microinjection, aliquots of cerebrospinal fluid were collected from the cisterna magna as reported previously (17). The whole brain was subsequently removed, and the left cerebrum, right cerebrum, and cerebellum were isolated and dissolved in 2.0 ml of 2 M NaOH at 60 °C for 1 h. The ^{125}I radioactivity of the samples was measured in a γ-counter (ART300, Aloka, Tokyo, Japan) for 3 min. The samples were then mixed with 14 ml of Hionic-fluor (Packard Instrument Co.), and ^{3}H radioactivity was measured in a liquid scintillation counter (TRI-CARB2050CA, Packard Instrument Co.) for 5 min. No radioactivity associated with this efflux transport process was detected in the contralateral cerebrum, cerebellum, or cerebrospinal fluid (data not shown), suggesting the operation of a selective efflux transport process across the BBB. The brain efflux index (BEI) was defined by the equation BEI % = (test substrate undergoing efflux at the BBB)/(test substrate injected into the brain) × 100, and the percentage of substrate remaining in the ipsilateral cerebrum was determined from 100 − BEI (%) = (amount of test substrate in the brain/amount of reference in the brain)/(amount of test substrate injected/amount of injected as a reference in the brain) × 100. The apparent elimination rate constant (k_e) was determined from the slope given by fitting a semilogarithmic plot of 100 − BEI *versus* time using the nonlinear least-squares regression analysis program MULTI (18).

^{125}I-Aβ$_{1-40}$ Plasma Pharmacokinetic Studies

Four or five 2- and 25-month-old mice in each group were anesthetized intramuscularly with a mixture of ketamine (125 mg/kg) and xylazine (1.22 mg/kg), and the jugular vein was isolated. Their body temperature was kept at 37 °C on a hot plate. Each mouse received a bolus intravenous injection of ^{125}I-Aβ$_{1-40}$ (5 μCi; 100 μl) into the jugular vein. Blood samples (30 μl) were collected from the tail vein by using a heparinized microcapillary at various intervals (1, 3, 5, 10, 15, 30, 60, 120, and 360 min) after the injection. The blood samples were centrifuged at 10,000 × *g* for 5 min at 4 °C, and the supernatant was obtained. To assess the integrity of the peptides, a plasma aliquot at each time point was cold-precipitated with 10% trichloroacetic acid in saline. After trichloroacetic acid precipitation, the precipitant was dissolved in 200 μl of 2 M NaOH at 55 °C for 10 min. The ^{125}I radioactivity of the samples was measured in a γ-counter (ART300) for 3 min.

The plasma concentration *versus* time data were analyzed by MOMENT (19) based on the model-independent moment analysis method (20). Briefly, the area under the plasma concentration-time curve (AUC) extrapolated to infinity was calculated the equation AUC = AUC_{0-360} + C_{360}/k_e, in which AUC_{0-360} is the area under the curve from time 0 to the time of the last plasma sample at 360 min calculated by the log-trapezoidal method, C_{360} is plasma concentration of the last plasma sample at 360 min, and k_e is the terminal elimination rate constant estimated from terminal points using the Akaike's Information Criterion-based method. The total body clearance (CLtot) was calculated by the equation CLtot = dose/AUC, where dose is the administered amount of ^{125}I-Aβ$_{1-40}$. The mean residence time (MRT) and the steady-state volume of distribution (Vdss) were calculated by MRT = AUMC/AUC and Vdss = CL·MRT, where AUMC is the total area under the first-moment time curve extrapolated to infinity.

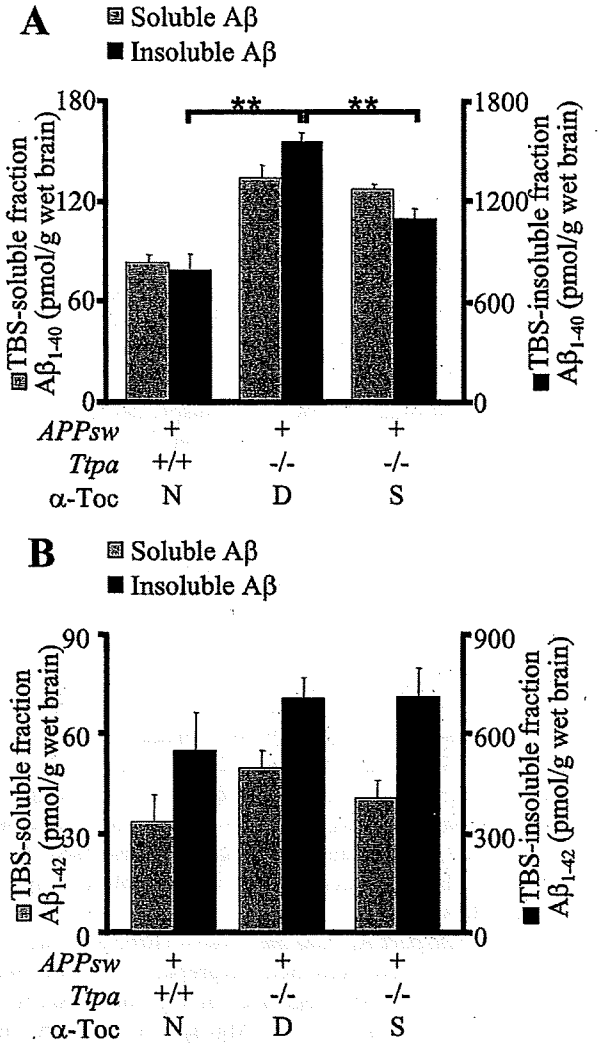

FIGURE 1. **The *Ttpa*$^{-/-}$*APPsw* mouse shows enhanced accumulation of Aβ in the brain.** *A* and *B*, cerebral Aβ$_{1-40}$ (*A*) and Aβ$_{1-42}$ (*B*) levels in 18-month-old mice. *Ttpa*$^{-/-}$*APPsw* mice showed increased level of Aβ$_{1-40}$ in the TBS-insoluble fraction of the brain homogenate and a similar tendency of increase of Aβ$_{1-40}$ and Aβ$_{1-42}$ in other fractions. This increase was partially ameliorated by α-Toc supplementation in the diet. *D*, α-Toc-deficient diet; *S*, α-Toc-supplemented diet; *N*, normal diet. **, $p < 0.01$.

Assay of Neprilysin-dependent Neutral Endopeptidase Activity

Four 4-month-old mice in each group were examined. Triton X-100-solubilized membrane fraction from brain was prepared to assay neutral endopeptidase activity as described previously (21). The neprilysin-dependent neutral endopeptidase activity was fluorometrically assayed using 0.1 mM succinyl-Ala-Ala-Phe-amidomethylcoumarin (Bachem, Bubendorf, Switzerland) as a substrate and determined from the fluorescence intensity (excitation, 390 nm; emission, 460 nm), based on the decrease in the rate of digestion caused by 0.1 μM thiorphan, a specific inhibitor of neprilysin.

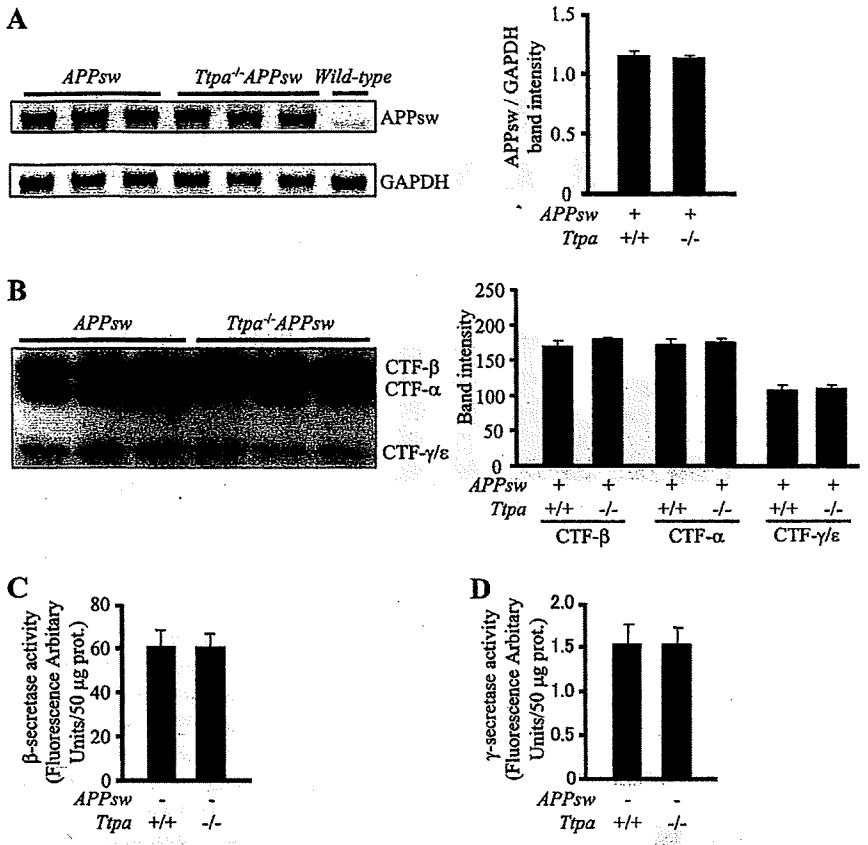

FIGURE 2. **α-Toc depletion does not increase APP expression nor β/γ-cleavages.** *A*, the human APPsw mRNA expression did not increase in the brains of *Ttpa*$^{-/-}$*APPsw* mice compared with *APPsw* mice. The band intensities normalized to the mouse glyceraldehyde-3-phosphate dehydrogenase (*GAPDH*) bands are shown in the *right panel*. *B*, protein levels of C-terminal fragments of APP-β, -α, and -γ/ε did not change in the brains of *Ttpa*$^{-/-}$*APPsw* mice compared with *APPsw* mice. Band intensities are shown in the *right panel*. *C* and *D*, the β (*C*)- and γ (*D*)-secretase activities did not increase in the brains of *Ttpa*$^{-/-}$ mice compared with wild-type mice.

Aβ Aggregation Study

Five 15-month-old *Ttpa*$^{-/-}$ mice and 10 age-matched wild-type mice were examined. Synaptosomes were prepared from mouse cerebrums as previously reported (22). Seed-free solutions of $A\beta_{1-40}$ were diluted with TBS. Aβ solutions at 50 μM were incubated at 37 °C with or without synaptosomes. Thioflavin T fluorescence intensities in the mixture incubated for 24 h were determined as previously described (23, 24).

Data Analysis

All data represent the average ± S.E. For multiple comparisons, single-factor analysis of variance followed by Fisher's protected least-significant-difference post hoc test was used. Results were considered statistically significant at $p < 0.05$.

RESULTS

Ttpa$^{-/-}$*APPsw Mouse Has an Enhanced Accumulation of Aβ in the Brain*—First, we biochemically studied the effect of α-Toc depletion on accumulation of Aβ. At 18 months, *Ttpa*$^{-/-}$*APPsw* mice showed markedly increased levels of $A\beta_{1-40}$ in the TBS-insoluble fraction of the brain homogenate and a similar tendency of increase of $A\beta_{1-40}$ and $A\beta_{1-42}$ in other fractions (Fig. 1, *A* and *B*). The *in vivo* accumulation of $A\beta_{1-40}$ was decreased when *Ttpa*$^{-/-}$*APPsw* mice were fed on the α-Toc-supplemented diet (Fig. 1*A*). An incomplete effect of α-Toc supplementation on accumulation of Aβ might be explained by the poor recruitment of supplemented α-Toc into the brain in *Ttpa*$^{-/-}$*APPsw* mice, because α-TTP in the brain transports α-Toc from blood to brain (7). This partial effect of α-Toc supplementation still could reduce accumulation of Aβ plaques (12).

APP Expression and β/γ Cleavages Are Not Increased—To examine the effect of α-Toc depletion on the metabolism of Aβ, we evaluated Aβ generation by measuring APP expression and secretase activities. The mRNA level of human APPsw in the brain did not increase in the brains of *Ttpa*$^{-/-}$*APPsw* mice compared with *APPsw* mice at 18 months of age (Fig. 2*A*). Moreover, protein levels of C-terminal fragments of APP-β, -α, and -γ/ε did not change in the brains of *Ttpa*$^{-/-}$*APPsw* mice compared with *APPsw* mice (Fig. 2*B*). This was supported by the *in vitro* results that β- and γ-secretase activities were not increased in the brains of 9-month-old *Ttpa*$^{-/-}$ mice (Fig. 2, *C* and *D*). These results indicate that the generation of Aβ in the brain of *Ttpa*$^{-/-}$*APPsw* mouse is not influenced by the depletion of α-Toc.

Aβ Clearance from the Brain Is Decreased in Ttpa$^{-/-}$ *Mice*—The increased Aβ accumulation without change of Aβ generation in *Ttpa*$^{-/-}$*APPsw* mouse brain led us to postulate that the increased Aβ accumulation by lipid peroxidation occurs through decreased Aβ clearance from the brain. Then we next directly studied Aβ clearance from the brain *in vivo* by using the BEI method (16, 17). We used *Ttpa*$^{-/-}$ mice in this experiment, because the injected ^{125}I-$A\beta_{1-40}$ should have been competed with endogenous Aβ, which accumulated in different degree in *Ttpa*$^{-/-}$*APPsw* and *APPsw* mouse brains, thereby complicating interpretation of the results. In contrast, *Ttpa*$^{-/-}$ mice have no detectable endogenous mouse Aβ in the brain. The ^{125}I-$A\beta_{1-40}$ was microinjected into the mouse cerebral cortex, and the remaining ^{125}I-$A\beta_{1-40}$ levels in the ipsilateral cerebrum were measured. The percentage of ^{125}I-$A\beta_{1-40}$ remaining at 60 min after injection was increased in 14-month-old *Ttpa*$^{-/-}$ mice compared with age-matched wild-type mice (Fig. 3*A*). The apparent elimination rate constant (k_e) was also markedly decreased because of α-Toc depletion (Fig. 3*B*). Although Aβ clearance decreases as a consequence of normal aging (25, 26), the reduction in k_e value evoked by α-Toc depletion (27.7%) was